Journal of Scientific Computing (2026) 107:30
https://doi.org/10.1007/s10915-026-03242-7

A conservative Mixed Finite Element Method for a Regularised Nonlinear Long-Wave Model

Ankur Ankur[1] · **Andrea Cangiani**[1] · **Ram Jiwari**[2]

Received: 26 November 2025 / Revised: 13 January 2026 / Accepted: 2 March 2026

Abstract
In this paper, we develop and analyze a mixed finite element method for a nonlinear, higher-order model describing nonlinear wave phenomena and exhibiting important conservation properties. A central goal of our approach is to ensure that these properties are preserved at the discrete level while avoiding the challenges typically encountered when constructing finite element subspaces of $H^2(\Omega)$ as would be required in a standard continuous Galerkin framework. At the continuous level, we establish well-posedness and characterize the solution through energy laws and mass conservation. For the semi-discrete formulation, we derive error estimates in various Bôchner spaces. Furthermore, we establish that the implicit fully discrete scheme is well-posed, converges with optimal order and consistent with both mass conservation and an entropy dissipation law. Finally, we confirm the theoretical findings and conservation properties on a set of benchmark problems.

Keywords KdV-RRLW model · Mixed Finite element method · Optimal error estimates · Fully discrete scheme · Existence and uniqueness

Mathematics Subject Classification 65N15 · 65N30

1 Introduction

Nonlinear wave phenomena are of great scientific importance and are notoriously difficult to resolve numerically. To date, numerous mathematical models have been proposed to characterize wave behaviors, such as the regularized long-wave (RLW) model [11], and the Korteweg-de Vries (KdV) model [13]. The KdV model is of critical importance in describing

✉ Ankur Ankur
aankur@sissa.it

Andrea Cangiani
andrea.cangiani@sissa.it

Ram Jiwari
ram1maths@gmail.com

[1] Mathematics Area, International School for Advanced Studies (SISSA), via Bonomea 265, I-34136 Trieste, Italy

[2] Department of Mathematics, Indian Institute of Technology Roorkee, 247667 Roorkee, India

the long wave propagation along any direction in some nonlinear dispersion systems. This model has also been used to describe several dynamical effects in longitudinal astigmatic waves and magnetic fluid waves. Although the KdV model was originally aimed at simulating water waves, it is now widely used to study a variety of different physical systems that exhibit long waves. However, this model is not always suitable for addressing wave-wave and wave-wall interactions. To illustrate this, another model was proposed by Rosenau [43], known as the Rosenau-regularised long-wave (RRLW) model.

The Korteweg-de Vries-Rosenau-regularised long-wave (KdV-RRLW) model is obtained by combining the KdV and RRLW models [1, 41]. It governs the dynamics of dispersive shallow water waves along lake shores and beaches. The high-order nature of the resulting PDE and the presence of nonlinear terms significantly complicate the numerical solution. Our goal is to address and overcome these inherent challenges.

1.1 Problem Description

The KdV-RRLW model for long-wave phenomena [1, 41] is based on the time-dependent fourth-order in space partial differential equation

$$w_t + \alpha\Delta^2 w_t - \beta\Delta w_t = \nabla\cdot(\boldsymbol{g}(w)) + \gamma\Delta w - \lambda\Delta^2 w \ \text{ in } \Omega_T, \tag{1.1}$$

where $\Omega_T = \Omega\times(0,T]$, and $\Omega\subseteq\mathbb{R}^d$ with $d\le 3$ is a convex and bounded domain. The model is equipped with initial data (ID) and boundary data (BD)

$$w(x,t) = 0 \ = \ \Delta w(x,t) \ \text{ for } (x,t)\in\partial\Omega\times(0,T], \tag{1.2}$$

$$w(x,0) = w_0(x), \ \text{ for } x\in\Omega. \tag{1.3}$$

The nonlinear function $\boldsymbol{g} = (g_i)_{i=1}^d$ is defined component-wise by

$$g_i(w) := -\Big(w + \frac{1}{s+1}w^{s+1}\Big), \ i=1,2,3; \ s\in\mathcal{S}, \quad \mathcal{S} = \begin{cases}\mathbb{N}, & \text{if } d=1,2,\\ \{1,2\}, & \text{if } d=3.\end{cases}$$

The first term on the left-hand side of (1.1) represents the linear temporal evolution. The parameters α and β correspond to the fifth- and third-order spatio-temporal dispersion terms, respectively, which are introduced to capture the equal-width effect of the evolving waves. The nonlinear term $\nabla\cdot(\boldsymbol{g}(w))$ consists of two components: the term $\nabla\cdot(w\mathbf{1})$ contributes to the drifting of the waves, while the second term models higher-order nonlinear dispersion effects. The coefficients α, β, λ, and γ are non-negative constants; in particular, γ accounts for dissipative effects, whereas λ introduces higher-order stabilization in the system. The restriction $s\in\{1,2\}$ imposed when $d=3$ guarantees the Sobolev embedding required in analysis; see e.g. (3.10).

Higher-order partial differential equations (PDEs) play an important role in many applications in science and engineering. Equation (1.1), with different values of α, β, γ and λ, occurs in a variety of physical applications. These include propagation of domain walls in liquid crystals [27], pattern formation in bi-stable systems [22], traveling waves in reaction-diffusion systems [2, 6], and mezoscopic model of phase-transition in binary systems near Lipschitz points [28].

The design and implementation of direct discretization of high-order PDEs is challenging. The H^2-conforming finite element method is the most direct way to discretize the problem (1.1)-(1.3). However, in its simplest, lowest order case, the implementation requires the use of a finite element space consisting of piecewise polynomials of degree five in two

dimensions and of order nine in three dimensions [46]. Additionally, such elements are typically not affine equivalent, necessitating the use of more complex methods to map the basis functions to each element using a reference element [19, 31, 32]; see [3] for an implementation based on Bernstein basis. Alternatively, one can employ nonconforming finite elements, such as cubic Hermite or Morley elements [19, 34], where the approximate solution lies in a finite-dimensional space that is not a subspace of $H^2(\Omega)$. Another alternative for solving fourth-order problems is the use of C^0 interior penalty methods [7, 14, 15]. These can be constructed at any order by incorporating parameter-dependent stabilizing terms on interior edges to weakly enforce flux continuity. Other techniques include [12, 29, 30, 45].

The mixed finite element method is an alternative approach to avoid using C^1 finite elements and, at the same time, reduce ill-conditioning. It is based on reducing the PDE order at the expense of introducing the Laplacian of the solution as a new variable [8, 10, 19]. This approach is highly attractive, at least for convex domains [37, 47]. By conforming to the continuous mixed formulation, the mixed finite element avoids the need for stabilizations. In this respect, it aligns with C^1-conforming methods. On the other hand, it is easier to implement and extend to higher orders. Indeed, both variables are approximated by classical H^1-conforming finite elements, thus bypassing the need for complex element constructions. Moreover, the mixed approach provides an approximation to the Laplacian of the solution simultaneously. Mixed formulations have been successfully employed in earlier works [24, 36], and more recently, Guo and co-workers [26] proposed a linear C^0 finite element scheme that simplifies implementation while maintaining the desired accuracy.

We propose the use of mixed FEM for the numerical solution of the KdV-RRLW problem. To the best of our knowledge, this allows for the first time to preserve the inherent mass conservation and, at the same time, satisfy a discrete energy dissipation inequality of the KdV-RRLW equation (and other related wave models) at the discrete level. Details of the significant contributions of this work are as follows:

- From a theoretical perspective, we establish well-posedness of the decoupled KdV-RRLW model. The analysis is based on using the Picard existence theorem and the Banach–Alaoglu theorem. The solution is characterized through mass conservation and energy laws, providing a solid foundation for both analytical and numerical studies.
- We derive semi-discrete error estimates in Bôchner space $L^\infty(0, T; H_0^1(\Omega))$ while showing that the numerical solution of the proposed mixed FEM converges to the exact solution with optimal order in the H^1 norm. The auxiliary variable also converges optimally in the L^2 norm.
- We also present a fully-discrete scheme, proving well-posedness and establishing rigorous error bounds. Importantly, the scheme preserves mass and satisfies a discrete energy dissipation law, confirming that fundamental physical properties of the model are maintained at the discrete level.
- Extensive numerical experiments validate the theoretical findings. The scheme accurately reproduces conservation properties and captures complex nonlinear wave phenomena, including 1D solitary waves, interaction of multiple waves, 2D undular bores, and Maxwellian-type initial conditions. Benchmark comparisons with existing methods demonstrate that the proposed approach achieves high accuracy and optimal convergence rates, confirming its robustness and effectiveness for simulating higher-order nonlinear wave models.

1.2 Structure of the Paper

This paper is organized as follows: Section 2 covers the weak formulation and key notations. In Section 3, we establish the well-posedness of the problem 1.1-(1.3) and characterize the solution through mass conservation and energy laws. Section 4 addresses the convergence of the semi-discrete problem in the $L^\infty(0,T;H_0^1(\Omega))$ norm. Section 5 discusses the full discretization of the problem using the Backward Euler method. Finally, Section 6 substantiates our theoretical findings with multiple examples and provides a comparison with other approaches.

2 Weak Formulation

We employ standard mathematical notations for Sobolev spaces and their norms. The norm in the Sobolev spaces $H^r(\mathcal{V})$, $\mathcal{V}\subset\mathbb{R}^3$, with $r\geq 1$ will be represented by $\|\cdot\|_{r,\mathcal{V}}$. The norm of $L^2(\mathcal{V})$, is simply denoted by $\|\cdot\|_{\mathcal{V}}$ and its inner product by $(\cdot,\cdot)_{\mathcal{V}}$. To make the notations clearer, we shall omit the subscript $\mathcal{V}$ in the inner product notations and norm when $\mathcal{V}=\Omega$. Let $H_0^1(\Omega)$ be the closure of $C_0^\infty(\Omega)$ in $\|\nabla\cdot\|$ norm and $C_0^\infty(\Omega)$ denotes the space of infinite differentiable functions with compact support in Ω.

Further, we use the Bôchner spaces $L^q(I;\mathcal{D})$ for $q\in\{1,2,\infty\}$ with the standard norm [42], where $\mathcal{D}$ is a Banach space and I is a suitable time interval. The symbols $K, C, K_i's$ and $C_i's$ with $i\in\mathbb{N}$ are utilized as constants. For the notation simplicity, we may use $\partial_t w$, w_t or $\dot{w}$ interchangeably in order to represent the temporal differentiation of w. Additionally, τ and h indicate the uniform step sizes in the time and space direction, respectively.
We introduce a new variable $z=-\Delta w$ to re-formulate the model (1.1)-(1.3) as follows:

$$\begin{cases} w_t-\alpha\Delta z_t+\beta z_t=\nabla\cdot\boldsymbol{g}(w)-\gamma z+\lambda\Delta z, & \text{in } \Omega_T,\\ w(x,0)=w_0(x) & \text{in } \Omega,\\ w=0 & \text{on } \partial\Omega, \end{cases} \quad \text{and} \quad \begin{cases} -\Delta w=z & \text{in } \Omega\times[0,T],\\ z=0 & \text{on } \partial\Omega. \end{cases} \tag{2.1}$$

Assuming $w_0\in H_0^1(\Omega)$, the weak form of the above mixed model reads: find $w,z\in L^2(0,T;H_0^1(\Omega))\cap C^0([0,T];H^1(\Omega))$ with $w_t,z_t\in L^2(0,T;H^1(\Omega))$ such that $\{w,z\}:[0,T]\to H_0^1(\Omega)\times H_0^1(\Omega)$ satisfy:

$$\begin{aligned}(w_t(t),\zeta)+\alpha(\nabla z_t(t),\nabla\zeta)+\beta(z_t(t),\zeta)&=(\nabla\cdot\boldsymbol{g}(w),\zeta)-\gamma(z(t),\zeta)\\ &\quad-\lambda(\nabla z(t),\nabla\zeta), \qquad \forall\,\zeta\in H_0^1(\Omega), t>0, \end{aligned}\tag{2.2a}$$

$$(\nabla w(t),\nabla\zeta')=(z(t),\zeta'), \qquad \forall\,\zeta'\in H_0^1(\Omega), t\geq 0, \tag{2.2b}$$

$$w(x,0)=w_0(x), \qquad \forall\, x\in\Omega. \tag{2.2c}$$

Note that (2.2b) also determines $z_0(x):=z(x,0)$ from w_0.

3 Well-Posedness of the Mixed Formulation

This section focuses on characterizing the solution via mass conservation and energy laws, as well as establishing the well-posedness of the weak formulation (2.2).

Lemma 3.1 (A priori bound) *If* (w, z) *solves* (2.2)*, then*

$$\|w(t)\|_1 + \|z(t)\| \leq \sqrt{2}\left[\|w_0\|_1 + \|z_0\|\right], \quad t \in (0, T], \tag{3.1}$$

In addition,

$$\|w\|_{L^\infty(L^q(\Omega))} \leq C_1, \quad \forall\, q \in \mathcal{S}_1, \quad \mathcal{S}_1 = \begin{cases} [1, \infty), & \text{if } d = 1, 2, \\ [1, 6], & \text{if } d = 3, \end{cases} \tag{3.2}$$

and

$$\|z(t)\|_1 \leq C_2, \quad t \in (0, T], \tag{3.3}$$

with $C_1, C_2 > 0$ *depending on the Sobolev embedding constant, and norms of* w_0, z_0*. Additionally,* C_2 *depends on* γ*,* λ*, final time* T*, and the Poincaré constant.*

Proof By selecting $\zeta = w$ in (2.2a) and $\zeta' = w, z$, and z_t (one at a time) in (2.2b) and utilizing the relation $(\nabla w_t(t), \nabla \zeta') = (z_t(t), \zeta')$, we obtain

$$(w_t, w) + \alpha(z_t, z) + \beta(\nabla w_t, \nabla w) = (\nabla \cdot \boldsymbol{g}(w), w) - \gamma\|\nabla w\|^2 - \lambda\|z\|^2. \tag{3.4}$$

Thus, we arrive at

$$\frac{C_3}{2}\frac{\mathrm{d}}{\mathrm{d}t}\left[\|w\|_1^2 + \|z\|^2\right] + \gamma\|\nabla w\|^2 + \lambda\|z\|^2 \leq \int_\Omega (\nabla \cdot \boldsymbol{g}(w)) w \, d\Omega. \tag{3.5}$$

where $C_3 := \min\{1, \alpha, \beta\}$. We define $\boldsymbol{F}(s) := \int_0^s \boldsymbol{g}(z)dz$ with $\boldsymbol{F}'(s) = \boldsymbol{g}(s), \quad s \in \mathbb{R}$ such that

$$\nabla \cdot \boldsymbol{F}(w) = \boldsymbol{g}(w) \cdot \nabla w. \tag{3.6}$$

Applying the divergence theorem noting that $w = 0$ on $\partial\Omega$ and $\boldsymbol{F}(0) = 0$ gives

$$\int_\Omega (\nabla \cdot \boldsymbol{g}(w)) w \, d\Omega = -\int_\Omega \boldsymbol{g}(w) \cdot \nabla w \, d\Omega = -\int_\Omega \nabla \cdot \boldsymbol{F}(w) \, d\Omega = -\int_{\partial\Omega} \boldsymbol{F}(w) \cdot \boldsymbol{n} \, dx = 0. \tag{3.7}$$

Using this in (3.5) and then integrating with respect to t results in

$$\frac{C_3}{2}\left[\|w\|_1^2 + \|z\|^2\right] + \gamma\int_0^t \|\nabla w(s)\|^2 ds + \lambda\int_0^t \|z(s)\|^2 ds \leq \frac{C_3}{2}\left[\|w_0\|_1^2 + \|z_0\|^2\right],$$

from which (3.1) readily follows given γ and λ are non-negative by assumption.

The estimate (3.2) holds by utilizing the Sobolev embedding [42] of $H^1(\Omega)$ in $L^q(\Omega)$, $q \in \mathcal{S}_1$. To prove the estimate (3.3), we select $\zeta = z$ in (2.2a), and $\zeta' = w_t$ in (2.2b), yielding

$$\frac{C_4}{2}\frac{\mathrm{d}}{\mathrm{d}t}\left[\|w\|_1^2 + \|z\|_1^2\right] \leq -(\boldsymbol{g}(w), \nabla z) - C_5\|z\|_1^2, \tag{3.8}$$

where $C_4 := \min\left\{\frac{1}{1+C_P}, \min\{\alpha, \beta\}\right\}$, $C_5 := \min\{\gamma, \lambda\}$ and C_P denotes the Poincaré constant. Leveraging the Young's and Cauchy-Schwarz inequalities, we obtain

$$\frac{C_4}{2}\frac{\mathrm{d}}{\mathrm{d}t}\left[\|w\|_1^2 + \|z\|_1^2\right] + \frac{C_5}{2}\|z\|_1^2 \leq \frac{1}{2C_5}(\|\boldsymbol{g}(w)\|^2). \tag{3.9}$$

Furthermore, using the bound (3.2) gives

$$\begin{aligned}\|\boldsymbol{g}(w)\|^2 &\le 3\int_\Omega \left(\frac{1}{s+1}w^{s+1}+w\right)^2 d\Omega \\ &\le \frac{6}{s+1}\int_\Omega w^{2s+2}d\Omega + 6\int_\Omega w^2 d\Omega \\ &\le 6|\Omega|\left(\frac{C_2^{2s+2}}{s+1}+C_2^2\right) := C_6, \end{aligned} \tag{3.10}$$

proving that $\boldsymbol{g} \in L^\infty(0,T;L^2(\Omega))$. Finally, integrating (3.9) with respect to time and using (3.10), we obtain

$$\|w(t)\|_1^2 + \|z(t)\|_1^2 \le \frac{C_6}{C_5C_4}T + \|w_0\|_1^2 + \|z_0\|_1^2, \tag{3.11}$$

and thus we conclude (3.3). □

Remark 3.2 (Physical interpretation) Lemma 3.1 establishes the stability of the system. It shows that the H^1-norm of the solution w and the L^2-norm of z (Laplacian of w) are controlled by the initial data.

Lemma 3.3 (Time-derivative bounds) *There exists a constant $C > 0$ such that, if (w,z) solves (2.2), then*

$$\|w_t(t)\|_1 + \|z_t(t)\|_1 \le C, \qquad t \in (0,T], \tag{3.12}$$

with $C > 0$ depending on the constants C_1 and C_2 from Lemma 3.1.

Proof Differentiating equation (2.2b) with respect to time yields

$$(\nabla w_t(t), \nabla\zeta') = (z_t(t), \zeta'), \qquad \forall\,\zeta' \in H_0^1(\Omega). \tag{3.13}$$

Next, by choosing $\zeta = z_t$ in equation (2.2a) and $\zeta' = w_t$ in (3.13), and then applying the Cauchy–Schwarz and Young inequalities, there exists a constant $C > 0$ such that

$$\|z_t(t)\|_1^2 + \|w_t(t)\|_1^2 \le C\big(\|\boldsymbol{g}(w)\|^2 + \|z(t)\|^2 + \|\nabla z(t)\|^2\big). \tag{3.14}$$

Finally, invoking the estimates obtained in equation (3.10) and Lemma 3.1 leads to the desired bound (3.12). □

Lemma 3.4 (Mass conservation) *Let (w,z) be a solution of (2.1) satisfying the no net flux boundary condition. Then the total mass is conserved in time, that is,*

$$M(t) := \int_\Omega w(x,t)\,dx = \int_\Omega w_0(x)\,dx \quad \textit{for all } t \ge 0. \tag{3.15}$$

Proof The result follows by testing the weak formulation of (2.1) with the constant function 1 and using the no net flux boundary condition to eliminate the boundary terms. □

Lemma 3.5 (Energy inequality) *Let (w,z) be a solution of (2.2). Then the following energy inequality holds:*

$$E(t) + \gamma\int_0^t \|\nabla w(s)\|^2\,ds + \lambda\int_0^t \|z(s)\|^2\,ds \;\le\; E(0), \tag{3.16}$$

where

$$E := E_1(w) + E_2(z) = \frac{\min\{1,\beta\}}{2}\|w(t)\|_1^2 + \frac{\alpha}{2}\|z(t)\|^2. \tag{3.17}$$

Proof The result follows by integrating equation (3.4) with respect to time t and proceeding as in the subsequent steps following (3.4). □

Theorem 3.6 (Existence and uniqueness) *Suppose $w_0 \in H_0^1(\Omega)$. Then, there exists a unique solution of the weak formulation (2.2) for any positive T.*

Proof We exploit the Faedo–Galerkin method (see [23, Chap. 7] and [20, 35]), dividing the proof into six parts as follows.

1. *Existence of local solutions:* Consider the finite dimensional subspace $\mathcal{G}^m = \text{span}\{\Psi_1, \Psi_2, \ldots, \Psi_m\}$, with $\{\Psi_j\}_{j=1}^{\infty}$ serving as an orthogonal basis for $H_0^1(\Omega)$. We introduce the functions $w^m, z^m : [0, T] \to H_0^1(\Omega)$, expressed as

$$w^m(t) = \sum_{j=1}^{m} a_m^j(t)\Psi_j \quad \text{and} \quad z^m(t) = \sum_{j=1}^{m} e_m^j(t)\Psi_j, \tag{3.18}$$

solution of

$$(w_t^m(t), \Psi_j) + \alpha(\nabla z_t^m(t), \nabla\Psi_j) + \beta(z_t^m(t), \Psi_j) = -(\boldsymbol{g}(w^m), \nabla\Psi_j) - \gamma(z^m(t), \Psi_j) - \lambda(\nabla z^m(t), \nabla\Psi_j), \tag{3.19a}$$

$$(\nabla w^m(t), \nabla\Psi_j) = (z^m(t), \Psi_j), \tag{3.19b}$$

where $w^m(0) = w_{0,m}$ and $\Psi_j \in \mathcal{G}^m$, $j = 1, 2, \ldots, m$.
Note that $w^m(0) = \sum_{j=1}^{m} e_m^j(0)\Psi_j$ and $e_m^j(0) = (w_0, \Psi_j)$. Upon substituting (3.18) into (3.19) we obtain the nonlinear system of ordinary differential equations

$$Q\dot{W}(t) + \alpha N\dot{P}(t) + \beta Q\dot{P}(t) = G(W(t)) - \gamma QP(t) - \lambda NP(t), \tag{3.20a}$$

$$Q^{-1}NW(t) = P(t), \tag{3.20b}$$

$$W(0) = W_0. \tag{3.20c}$$

Where,

$$\begin{aligned} Q &= [Q_{ij}]_{m\times m},\ Q_{ij} = (\Psi_i, \Psi_j),\ i, j = 1, 2\ldots m,\\ N &= [N_{ij}]_{m\times m},\ N_{ij} = (\nabla\Psi_i, \nabla\Psi_j),\ i, j = 1, 2\ldots m,\\ W(t) &= (a_m^1(t), a_m^2(t)\ldots, a_m^m(t))^T,\ P(t) = (e_m^1(t), e_m^2(t)\ldots, e_m^m(t))^T,\\ W_0 &= (a_m^1(0), a_m^2(0)\ldots, a_m^m(0))^T,\\ G(W) &= (G_j) \text{ where } G_j = -(\boldsymbol{g}(w^m), \nabla\Psi_j). \end{aligned}$$

Since matrices Q and N are symmetric and positive definite, their inverses exist. Using (3.20b) in (3.20a), nonlinear system (3.20) reduces to

$$Q[I + \alpha(Q^{-1}N)^2 + \beta Q^{-1}N]\ \dot{W}(t) = G(W(t)) - \gamma NW(t) - \lambda NQ^{-1}NW(t), \tag{3.21a}$$

$$W(0) = W_0. \tag{3.21b}$$

Finally, we have

$$\dot{W}(t) = \left[[I + \alpha(Q^{-1}N)^2 + \beta Q^{-1}N]^{-1}Q^{-1}\right]\left[G(W(t)) - \gamma NW(t) - \lambda NQ^{-1}NW(t)\right], \tag{3.22a}$$

$$W(0) = W_0. \tag{3.22b}$$

By applying the Picard existence theorem, we ensure the existence of a local solution $(w^m(t), z^m(t))$ in the subspace $\mathcal{G}^m \times \mathcal{G}^m$ on $[0, T^*]$ for some $0 < T^* < T$. To extend this solution up to the final time T, it suffices to rule out finite-time blow-up. Classical ODE theory ensures that a maximal existence time $T^* < T$ can occur only if the relevant solution norms become unbounded as $t \to T^{*-}$. Hence, in what follows, we derive uniform bounds that prevent such blow-up, allowing continuation of the solution from T^* to T.

2. *Uniform-bounds.* For $j = 1, 2, \ldots, m$, multiplying (3.19a) by $a_m^j(t)$ and (3.19b) by $a_m^j(t)$,$e_m^j(t)$ and $e_{m,t}^j(t)$ (one at a time) and then summing over j yields

$$\frac{C}{2}\frac{\mathrm{d}}{\mathrm{d}t}\big[\|w^m(t)\|_1^2 + \|z^m(t)\|^2\big] + \gamma\|\nabla w\|^2 + \lambda\|z\|^2 \le (\nabla \cdot \boldsymbol{g}(w^m), w^m(t)),$$

for some $C > 0$. Proceeding analogously to the proof of Lemma 3.1 and taking the supremum over $0 \le t \le T$, while noting that $\|w^m(0)\|_1 \le \|w_0\|_1$ and $\|z^m(0)\| \le \|z_0\|$, we obtain

$$\sup_{0\le t\le T}\|w^m(t)\|_1^2 + \gamma\int_0^T \|\nabla w^m(t)\|^2 dt + \lambda\int_0^T \|z^m(t)\|^2 dt \le C. \tag{3.23}$$

Following similar arguments as in Lemmas 3.1 and 3.3 we further derive the uniform bounds

$$\sup_{0\le t\le T}\|z^m(t)\|_1^2 + \int_0^T \|z^m(t)\|_1^2 dt \le C,$$
$$\int_0^T \|w_t^m(t)\|_1^2 dt + \int_0^T \|z_t^m(t)\|_1^2 dt \le C,$$

preventing finite-time blow-up. Thus, by the continuation argument, the Galerkin solution $(w^m(t), z^m(t))$ exists on the entire interval $[0, T]$.

3. *Passing limit inside.* Invoking the Banach–Alaoglu theorem [16, 18], we obtain subsequences with

$$\begin{aligned}
z^{m_k} &\xrightarrow{w^*} z \ \ in \ \ L^\infty(0,T;H_0^1(\Omega)),\\
w^{m_k} &\xrightarrow{w^*} w \ \ in \ \ L^\infty(0,T;H_0^1(\Omega)),\\
w_t^{m_k} &\xrightarrow{w} w_t \ \ in \ \ L^2(0,T;H^1(\Omega)),\\
z_t^{m_k} &\xrightarrow{w} z_t \ \ in \ \ L^2(0,T;H^1(\Omega)).
\end{aligned} \tag{3.24}$$

By the Aubin–Lions compactness lemma [44], the subsequence $\{w^{m_k}\}$ converges strongly to w, i.e.,

$$w^{m_k} \longrightarrow w \ \ in \ \ L^2(0,T;L^2(\Omega)). \tag{3.25}$$

Next, we shall use the convergence of subsequences $\{w^{m_k}\}_{k=1}^\infty$ and $\{z^{m_k}\}_{k=1}^\infty$ to pass the limit inside equation (3.19). To facilitate this process, define $\zeta, \zeta' \in C^1([0,T]; H_0^1(\Omega))$ as

$$\zeta(t) = \sum_{j=1}^M a^j(t)\Psi_j \quad \text{and} \quad \zeta'(t) = \sum_{j=1}^M e^j(t)\Psi_j,$$

with $\{a^j(t)\}_{j=1}^M$ and $\{e^j(t)\}_{j=1}^M$ smooth functions.

For $m \geq M$, we multiply (3.19a) by $a^j(t)$ and (3.19b) by $e^j(t)$, take sum over j from 1 to M, and then integrate to yield

$$\int_0^T \Big[(w_t^m(t), \zeta(t)) + \alpha(\nabla z_t^m(t), \nabla\zeta(t)) + \beta(z_t^m(t), \zeta(t))\Big]dt = \int_0^T \Big[(\nabla \cdot \boldsymbol{g}(w^m), \zeta(t)) - \gamma(z^m(t), \zeta(t)) - \lambda(\nabla z^m(t), \nabla\zeta(t))\Big]dt, \tag{3.26a}$$

$$\int_0^T \Big[(\nabla w^m(t), \nabla\zeta'(t))\Big]dt = \int_0^T \Big[(z^m(t), \zeta'(t))\Big]dt. \tag{3.26b}$$

Choosing $m = m_k$ and using (3.24) and (3.25), we obtain

$$\int_0^T \Big[(w_t(t), \zeta(t)) + \alpha(\nabla z_t(t), \nabla\zeta(t)) + \beta(z_t(t), \zeta(t))\Big]dt = \int_0^T \Big[(\nabla \cdot \boldsymbol{g}(w), \zeta(t)) - \gamma(z(t), \zeta(t)) - \lambda(\nabla z(t), \nabla\zeta(t))\Big]dt, \tag{3.27a}$$

$$\int_0^T \Big[(\nabla w(t), \nabla\zeta'(t))\Big]dt = \int_0^T \Big[(z(t), \zeta'(t))\Big]dt. \tag{3.27b}$$

Finally, employing a density argument, we can assert that equation (2.2) holds true for $\zeta, \zeta' \in H_0^1(\Omega)$ almost everywhere in the interval $[0, T]$.

4. *Initial data.* Lastly, we are left showing that $w(0) = w_0$. Using equation (3.27a) with $\zeta \in C^1([0, T]; H_0^1(\Omega))$ such that $\zeta(T) = 0$, it follows that

$$\int_0^T \Big[(-w(t), \zeta_t(t)) + \alpha(\nabla z_t(t), \nabla\zeta(t)) + \beta(z_t(t), \zeta(t))\Big]dt = \int_0^T \Big[(\nabla \cdot \boldsymbol{g}(w), \zeta(t)) - \gamma(z(t), \zeta(t)) - \lambda(\nabla z(t), \nabla\zeta(t))\Big]dt + (w(0), \zeta(0)). \tag{3.28}$$

Similarly, (3.26a) yields

$$\int_0^T \Big[(-w^m(t), \zeta_t(t)) + \alpha(\nabla z_t^m(t), \nabla\zeta(t)) + \beta(z_t^m(t), \zeta(t))\Big]dt = \int_0^T \Big[(\nabla \cdot \boldsymbol{g}(w^m), \zeta(t)) - \gamma(z^m(t), \zeta(t)) - \lambda(\nabla z^m(t), \nabla\zeta(t))\Big]dt + (w^m(0), \zeta(0)). \tag{3.29}$$

Choosing $m = m_k$ and applying (3.24) and (3.25) while noting that $w^m(0) \to w_0$ as $m \to \infty$, we obtain

$$\int_0^T \Big[(-w(t), \zeta_t(t)) + \alpha(\nabla z_t(t), \nabla\zeta(t)) + \beta(z_t(t), \zeta(t))\Big]dt = \int_0^T \Big[(\nabla \cdot \boldsymbol{g}(w), \zeta(t)) - \gamma(z(t), \zeta(t)) - \lambda(\nabla z(t), \nabla\zeta(t))\Big]dt + (w_0, \zeta(0)). \tag{3.30}$$

With $\zeta(0)$ being arbitrary, a simple comparison of (3.28) with (3.30) allows us to conclude that $w(0) = w_0$.

5. *Uniqueness.* Suppose (w_1, z_1) and (w_2, z_2) are two different solutions to the mixed weak formulation (2.2). Introducing $V := w_1 - w_2$ and $X := z_1 - z_2$ leads to

$$(V_t(t), \zeta) + \alpha(\nabla X_t(t), \nabla\zeta) + \beta(X_t(t), \zeta) = -(\boldsymbol{g}(w_1) - \boldsymbol{g}(w_2), \nabla\zeta) - \gamma(X(t), \zeta) - \lambda(\nabla X(t), \nabla\zeta), \zeta), \tag{3.31a}$$

$$(\nabla V(t), \nabla\zeta') = (X(t), \zeta'), \tag{3.31b}$$

$$V(0) = 0, X(0) = 0. \tag{3.31c}$$

Taking $\zeta = V$ in (3.31a) and $\zeta' = X_t$, V and X (one at a time) in (3.31b), we get

$$(V_t(t), V(t)) + \alpha(X_t(t), X(t)) + \beta(\nabla V_t(t), \nabla V(t)) = -\gamma\|\nabla V(t)\|^2 - \lambda\|X(t)\|^2 - (\boldsymbol{g}(w_1) - \boldsymbol{g}(w_2), \nabla V(t)). \tag{3.32a}$$

Here, we have used the identity $(\nabla V_t(t), \nabla V) = (X_t(t), V(t))$. Now, the Young's and Cauchy–Schwarz inequalities and the Lipschitz continuity of function g yield

$$\frac{\mathrm{d}}{\mathrm{d}t}\big[\|V(t)\|_1^2 + \|X(t)\|^2\big] \le C\|V(t)\|_1^2.$$

Integration w.r.t. time yields

$$\|V(t)\|_1^2 + \|X(t)\|^2 \le \|V(0)\|_1^2 + \|X(0)\|^2 + C\int_0^t \|V(s)\|_1^2 ds.$$

Thus, Gronwall's lemma implies that

$$\|V(t)\|_1^2 \le e^{Ct}\big(\|V(0)\|_1^2 + \|X(0)\|^2\big) = 0.$$

Hence, $w_1 = w_2$ and using (3.31b), we conclude that $z_1 = z_2$.

□

4 Semidiscrete Error Estimates of Mixed Formulation

We consider here a spatially discrete scheme. The a priori analysis is based classically on the Ritz projection operator.

Let Ω be partitioned by a shape-regular family of triangulations $\{\mathcal{T}_h\}_{h>0}$ with mesh size $h = \max_{K\in\mathcal{T}_h} \mathrm{diam}(K)$. Let $S_h \subset H_0^1(\Omega)$ be a finite-element subspace defined on this mesh, satisfying the following standard approximation properties for some $m \ge 1$: There exists a constant $C > 0$ such that, if $w \in H^r(\Omega) \cap H_0^1(\Omega)$, for $1 \le r \le m$, then

$$\inf_{\zeta\in S_h}\{\|w - \zeta\| + h\|\nabla(w - \zeta)\|\} \le Ch^r\|w\|_r. \tag{4.1}$$

We also define the Ritz operator $\Pi_h : H_0^1(\Omega) \to S_h$, which is determined by solving

$$(\nabla\Pi_h w, \nabla\zeta) = (\nabla w, \nabla\zeta) \quad \forall\zeta \in S_h, \quad w \in H_0^1(\Omega), \tag{4.2a}$$

$$(\nabla\Pi_h z, \nabla\zeta') = (\nabla z, \nabla\zeta') \quad \forall\zeta' \in S_h, \quad z \in H_0^1(\Omega). \tag{4.2b}$$

Setting $\zeta = \Pi_h w$, we observe that $\|\nabla \Pi_h w\| \leq \|\nabla w\|, \ \forall w \in H_0^1(\Omega)$. Further, we readily verify that

$$\|\Pi_h w - w\| + h\|\nabla(\Pi_h w - w)\| \leq Ch^r \|w\|_r, \tag{4.3a}$$

$$\|\Pi_h z - z\| + h\|\nabla(\Pi_h z - z)\| \leq Ch^r \|z\|_r, \tag{4.3b}$$

for each $w, z \in H^r(\Omega) \cap H_0^1(\Omega)$ and $1 \leq r \leq m$.

Finally, defining $w_0^h = \Pi_h w_0$, the semi-discretisation of (1.1)-(1.3) is formulated as follows. Find $w^h, z^h : [0, T] \to S_h$ satisfying

$$(w_t^h(t), \zeta) + \alpha(\nabla z_t^h(t), \nabla\zeta) + \beta(z_t^h(t), \zeta) = (\nabla \cdot \boldsymbol{g}(w^h) - \gamma(z^h(t), \zeta), \zeta) - \lambda(\nabla z^h(t), \nabla\zeta), \quad \zeta \in S_h, t > 0, \tag{4.4a}$$

$$(\nabla w^h(t), \nabla\zeta') = (z^h(t), \zeta'), \quad \zeta' \in S_h, t \geq 0, \tag{4.4b}$$

$$w^h(0) = w_0^h. \tag{4.4c}$$

Since S_h is finite dimensional, the above system of equations reduces to a system of nonlinear ODEs. By Picard's theorem, there exists a unique local solution on interval $(0, t^*)$ for some $t^* > 0$. To extend this solution globally in time, we exploit again a continuation argument. To this end, we first derive the following a priori bound.

Lemma 4.1 (A priori bound) *If* (w^h, z^h) *satisfies* (4.4)*, then*

$$\|w^h(t)\|_1 \leq \|w_0^h\|_1 + \|z_0^h\|, \quad t \in (0, T]. \tag{4.5}$$

In addition

$$\|w^h\|_{L^\infty(L^q(\Omega))} \leq C, \quad \forall\, q \in \mathcal{S}_1, \quad \mathcal{S}_1 = \begin{cases} [1, \infty), & \text{if } d = 1, 2, \\ [1, 6], & \text{if } d = 3, \end{cases} \tag{4.6}$$

where $C > 0$ *depends on the Sobolev embedding constant, and norms of* w_0, z_0.

Proof Substituting $\zeta = w^h$ in (4.4a) and $\zeta' = w^h, z^h$ and z_t^h (one at a time) in (4.4b), we obtain

$$\frac{C}{2}\frac{\mathrm{d}}{\mathrm{d}t}\Big[\|w^h\|_1^2 + \|z^h\|^2\Big] + \gamma\|\nabla w^h\|^2 + \lambda\|z^h\| \leq \int_\Omega (\nabla \cdot \boldsymbol{g}(w^h)) w^h d\Omega. \tag{4.7}$$

Using equation (3.7) in (4.7) with non-negative γ and λ, we get

$$\frac{\mathrm{d}}{\mathrm{d}t}\Big[\|w^h\|_1^2 + \|z^h\|^2\Big] \leq 0,$$

and thus, integrating with respect to time t yields

$$\|w^h\|_1^2 + \|z^h\|^2 \leq \|w_0^h\|_1^2 + \|z_0^h\|^2,$$

implying (4.5). In turn, the bound (4.6) follows immediately by the Sobolev embedding [42] of $H^1(\Omega)$ in $L^q(\Omega)$ for $q \in \mathcal{S}_1$. □

Theorem 4.2 *Let* (w, z) *be the solution of the weak formulation (2.2) and* (w^h, z^h) *be the solution to the semidiscrete scheme (4.4). Assume that* $w \in L^\infty(0, T; H_0^1(\Omega))$

$\cap L^2(0,T;H^r(\Omega))$ *with* $w_t \in L^2(0,T;H^r(\Omega))$, $z \in L^\infty(0,T;H_0^1(\Omega)) \cap L^\infty(0,T;H^r(\Omega))$ *with* $z_t \in L^2(0,T;H^r(\Omega))$, *and* $z(0) \in H^r(\Omega)$. *Then, the following a priori estimate holds:*

$$h\|w - w^h\|_{L^\infty(0,T;H_0^1(\Omega))} + \|z - z^h\|_{L^\infty(0,T;L^2(\Omega))} \leq Ch^r\, \mathcal{Q}_r, \tag{4.8}$$

where C denotes a positive constant independent of h and

$$\mathcal{Q}_r := \|z\|_{L^\infty(0,T;H^r(\Omega))} + \|z(0)\|_{H^r(\Omega)} + \|z_t\|_{L^2(0,T;H^r(\Omega))} + \|w\|_{L^2(0,T;H^r(\Omega))} + \|w_t\|_{L^2(0,T;H^r(\Omega))}.$$

Proof The error can be expressed as

$$w(t) - w^h(t) = (w(t) - \Pi_h w(t)) + (\Pi_h w(t) - w^h(t)) = \varrho(t) + \vartheta(t),$$
$$z(t) - z^h(t) = (z(t) - \Pi_h z(t)) + (\Pi_h z(t) - z^h(t)) = \mu(t) + \varphi(t).$$

In cases where there is no ambiguity, we will write $\vartheta(t)$ in place of ϑ, and follow the same approach for ϱ, μ, and φ.

Subtracting (4.4) from (2.2) while utilizing the Ritz projection Π_h, we arrive at

$$(\vartheta_t, \zeta) + \alpha(\nabla\varphi_t, \nabla\zeta) + \beta(\varphi_t, \zeta) + \gamma(\varphi, \zeta) + \lambda(\nabla\varphi, \nabla\zeta) = -(\varrho_t, \zeta) - \beta(\mu_t, \zeta) - \gamma(\mu, \zeta) - (\boldsymbol{g}(w) - \boldsymbol{g}(w^h), \nabla\zeta), \tag{4.9a}$$

$$(\nabla\vartheta, \nabla\zeta') = (\mu, \zeta') + (\varphi, \zeta'). \tag{4.9b}$$

Setting $\zeta' = \varphi_t$, ϑ and φ (one at a time) in (4.9b) and using the resulting equations in (4.9a) together with $\zeta = \vartheta$, gives

$$(\vartheta_t, \vartheta) + \alpha(\varphi, \varphi_t) + \beta(\nabla\vartheta_t, \nabla\vartheta) + \gamma(\nabla\vartheta, \nabla\vartheta) + \lambda(\varphi, \varphi) = -(\varrho_t, \vartheta) - \lambda(\mu, \varphi) - \alpha(\mu, \varphi_t) - (\boldsymbol{g}(w) - \boldsymbol{g}(w^h), \nabla\vartheta).$$

Thus,

$$\frac{C}{2}\frac{\mathrm{d}}{\mathrm{d}t}\left[\|\vartheta(t)\|_1^2 + \|\varphi(t)\|^2\right] + \gamma\|\nabla\vartheta(t)\|^2 + \lambda\|\varphi(t)\|^2 \leq -(\varrho_t, \vartheta) - \lambda(\mu, \varphi) - \alpha(\mu, \varphi_t) - (\boldsymbol{g}(w) - \boldsymbol{g}(w^h), \nabla\vartheta), \tag{4.10}$$

where $C = min\{1, \alpha, \beta\}$. The Cauchy–Schwarz and Young's inequalities, equation (4.9b) with $\zeta' = \vartheta$ gives

$$\|\nabla\vartheta(t)\|^2 \leq C\big(\|\varphi(t)\|^2 + \|\mu(t)\|^2 + \|\vartheta(t)\|^2\big). \tag{4.11}$$

Using (4.11) in (4.10) yields

$$\frac{\mathrm{d}}{\mathrm{d}t}\left[\|\varphi(t)\|^2 + \|\vartheta(t)\|_1^2\right] \leq C\big(\|\mu(t)\|^2 + \|\vartheta(t)\|^2 + \|\varphi(t)\|^2 + \|\varrho(t)\|^2 + \|\varrho_t(t)\|^2\big) - \alpha\,\partial_t(\mu, \varphi) + \alpha(\mu_t, \varphi).$$

Here, we have used once again the Cauchy–Schwarz and Young's inequalities and the Lipschitz continuity of g. Next, integrating with respect to time t and recalling that estimate (4.11) holds also at $t = 0$ yields

$$\|\vartheta(t)\|_1^2 + \|\varphi(t)\|^2 \leq C\Big(\|\mu(t)\|^2 + \|\varphi(0)\|^2 + \|\mu(0)\|^2 + \|\vartheta(0)\|^2$$

$$+\int_0^T \left(\|\vartheta(t)\|^2+\|\mu(t)\|^2+\|\varphi(t)\|^2+\|\varrho(t)\|^2+\|\varrho_t(t)\|^2+\|\mu_t(t)\|^2\right)\Big). \tag{4.12}$$

Now, evaluating (4.9b) at time $t=0$ and substituting $\zeta'=\varphi(0)$ together with $\vartheta(0)=0$, we arrive at

$$\|\varphi(0)\|^2 \le \frac{1}{2}\|\varphi(0)\|^2+\frac{1}{2}\|\mu(0)\|^2,$$

and hence, we get

$$\|\varphi(0)\|^2 \le Ch^{2r}\|z(0)\|_r^2. \tag{4.13}$$

Applying the Gronwall's lemma on (4.12) while using the given hypothesis, estimates (4.3a) and (4.3b) and equation (4.13), we obtain

$$\|\vartheta(t)\|_1^2+\|\varphi(t)\|^2 \le Ch^{2r}. \tag{4.14}$$

Ultimately, we arrive at the estimate (4.8) by combining equations (4.14) with (4.3a) and (4.3b) while considering the supremum across $0\le t\le T$. □

5 Full Discretization

We finally introduce and analyze a full discretisation of the problem (2.2). Let M be a positive integer representing the number of time steps with $\tau=\frac{T}{M}$ indicating the duration of each time interval and $t^j=j\tau$, for $j=0,1,\ldots,M$, the discrete time instances. For any function $\eta\in C\big(I;L^2(\Omega)\big)$, we define

$$\eta^j=\eta(t^j) \quad\text{and}\quad \delta_t\eta^j=\frac{\eta^j-\eta^{j-1}}{\tau}, \quad \forall\ j=1,\ldots,M. \tag{5.1}$$

We propose a fully discrete finite element approximation for problem (4.4) based on the Backward Euler time-stepping as follows. Find $W=(W^j)_{j=0}^M$ and $Z=(Z^j)_{j=0}^M$ with $(W^j,Z^j)\in S_h\times S_h$ such that

$$(\delta_t W^j,\zeta)+\alpha(\nabla\delta_t Z^j,\nabla\zeta)+\beta(\delta_t Z^j,\zeta)=-\lambda(\nabla Z^j,\nabla\zeta)+(\nabla\cdot\boldsymbol{g}(W^j),\zeta)-\gamma(Z^j,\zeta), \quad \forall\ j=1,\ldots,M, \tag{5.2a}$$

$$(\nabla W^j,\nabla\zeta')=(Z^j,\zeta'), \quad \forall\ j=0,1,\ldots,M, \tag{5.2b}$$

$$W^0=w_0^h. \tag{5.2c}$$

Once again, we start the analysis by establishing an a priori bound.

Lemma 5.1 (A priori bound) *If (W,Z) satisfies (5.2). then,*

$$\|W^j\|_1+\|Z^j\| \le \sqrt{2}(\|W^0\|_1+\|Z^0\|), \tag{5.3}$$

for $j=1,\ldots,M$ and, moreover,

$$\|W^j\|_{L^q(\Omega)}\le C, \quad \forall\ q\in\mathcal{S}_1, \quad \mathcal{S}_1=\begin{cases}[1,\infty), & \text{if } d=1,2,\\ [1,6], & \text{if } d=3,\end{cases} \tag{5.4}$$

for some constant $C>0$.

Proof Testing with $\zeta = W^j$ in (5.2a) and with $\zeta' = W^j, Z^j$, and $\delta_t Z^j$ (one at a time) in (5.2b), we obtain

$$\left(\frac{W^j - W^{j-1}}{\tau}, W^j\right) + \alpha\left(\frac{Z^j - Z^{j-1}}{\tau}, Z^j\right) + \beta\left(\nabla\left(\frac{W^j - W^{j-1}}{\tau}\right), \nabla W^j\right) + \lambda\|Z^j\| + \gamma\|\nabla W^j\| = (\nabla \cdot \boldsymbol{g}(W^j), W^j). \tag{5.5}$$

Applying the Cauchy–Schwarz and Young's inequalities together with equation (3.7) in (5.5), we get

$$\delta_t\left[\|W^j\|_1^2 + \|Z^j\|^2\right] \leq 0,$$

as $\lambda, \gamma > 0$, and, summing the above bounds from 1 to j, already provides (5.3). From this, the bound (5.4) immediately follows by Sobolev embedding [42]. □

Testing the fully discrete scheme as done in the continuous case, cf. Lemma 3.4, with the constant function 1 immediately yields the following mass conservation result.

Lemma 5.2 (Mass conservation) *Assume that (W, Z) is a solution of the fully discrete scheme (5.2) opportunely modified to satisfy (2.1) with no net flux boundary conditions. Then the following conservation law holds true for $j = 0, \ldots, M$:*

$$M(W^j) := \int_\Omega W^j \, dx = \int_\Omega W^0 \, dx. \tag{5.6}$$

Lemma 5.3 (Energy inequality) *Assume that (W, Z) is a solution of the fully discrete scheme (5.2). Then the following discrete energy inequality holds true for $j = 1, \ldots, M$:*

$$E(W^j, Z^j) + \gamma\tau \sum_{i=1}^{j} \|\nabla W^i\|^2 + \lambda\tau \sum_{i=1}^{j} \|Z^i\|^2 \leq E(W^0, Z^0), \tag{5.7}$$

where

$$E(W^j, Z^j) = E(W^j) + E(Z^j) = \frac{\min\{1, \beta\}}{2}\|W^j\|_1^2 + \frac{\alpha}{2}\|Z^j\|^2. \tag{5.8}$$

Proof The result follows from equation (5.5) by applying the Cauchy–Schwarz and Young inequalities and subsequently summing over the time steps 1 through j. □

We now aim to establish the existence and uniqueness of the fully discrete solution W^j by applying the Brouwer fixed point theorem (see [25, Chap. IV, Corollary 1.1]; see also [20, 38]).

Theorem 5.4 *Let $1 < j \leq M$ and suppose $(W^0, Z^0), (W^1, Z^1), \ldots, (W^{j-1}, Z^{j-1})$ are given satisfying 5.2. Then, (W^j, Z^j) exists and it satisfies (5.2) uniquely.*

Proof We define an inner product and corresponding norm on the space $S_h \times S_h$:

$$\left(\psi, \psi'\right)_{S_h \times S_h} = \left(\psi_1, \psi_1'\right)_{S_h} + \left(\psi_2, \psi_2'\right)_{S_h},$$

$$\|\psi\|_{S_h \times S_h}^2 = \|\psi_1\|_{S_h}^2 + \|\psi_2\|_{S_h}^2,$$

with $\psi = (\psi_1, \psi_2)$ and $\psi' = (\psi_1', \psi_2')$.
Consider $\mathcal{H} = [\mathcal{H}_1, \mathcal{H}_2]$ over the space $S_h \times S_h$, where the mappings $\mathcal{H}_1, \mathcal{H}_2 : S_h \times S_h \to S_h$ are defined to satisfy

$$(\mathcal{H}_1(\psi), \zeta)_{S_h} = (\psi_1, \zeta)_{S_h} + \alpha(\nabla\psi_2, \nabla\zeta)_{S_h} + \beta(\nabla\psi_1, \nabla\zeta)_{S_h}$$

$$
\begin{aligned}
&- (W^{j-1}, \zeta)_{S_h} - \alpha(\nabla Z^{j-1}, \nabla\zeta)_{S_h} - \beta(\nabla W^{j-1}, \nabla\zeta)_{S_h} \\
&+ \tau\big[(\boldsymbol{g}(\psi_1), \nabla\zeta)_{S_h} + \gamma(\nabla\psi_1, \nabla\zeta)_{S_h} + \lambda(\nabla\psi_2, \nabla\zeta)_{S_h}\big], \quad \forall\, \zeta \in S_h,
\end{aligned} \tag{5.9a}
$$

$$
(\mathcal{H}_2(\psi), \zeta')_{S_h} = (\tau\lambda + \alpha)\big[(\psi_2, \zeta')_{S_h} - (\nabla\psi_1, \nabla\zeta')_{S_h}\big]. \tag{5.9b}
$$

It is straightforward to see that $\mathcal{H}$ maintains continuity. Now, substituting $(\zeta, \zeta') = (\psi_1, \psi_2)$ yields

$$
\begin{aligned}
(\mathcal{H}(\psi), \psi)_{S_h\times S_h} &= (\mathcal{H}_1(\psi), \psi_1)_{S_h} + (\mathcal{H}_2(\psi), \psi_2)_{S_h}, \\
&\geq C\|\psi\|^2_{S_h\times S_h} - (W^{j-1}, \psi_1)_{S_h} - \alpha(\nabla Z^{j-1}, \nabla\psi_1)_{S_h} \\
&\quad - \beta(\nabla W^{j-1}, \nabla\psi_1)_{S_h} + (\beta + \tau\gamma)\|\nabla\psi_1\|^2_{S_h},
\end{aligned}
$$

leading to

$$
\begin{aligned}
(\mathcal{H}(\psi), \psi)_{S_h\times S_h} &\geq C\|\psi\|^2_{S_h\times S_h} - \frac{1}{2C}\|W^{j-1}\|^2_{S_h} - \frac{C}{2}\|\psi_1\|^2_{S_h} - \frac{\alpha^2}{4\beta}\|\nabla Z^{j-1}\|^2_{S_h} - \frac{\beta^2}{4\tau\gamma}\|\nabla W^{j-1}\|^2_{S_h} \\
&\geq \frac{C}{2}\|\psi\|^2_{S_h\times S_h} - \frac{1}{2C}\|W^{j-1}\|^2_{S_h} - \frac{\alpha^2}{4\beta}\|\nabla Z^{j-1}\|^2_{S_h} - \frac{\beta^2}{4\tau\gamma}\|\nabla W^{j-1}\|^2_{S_h}.
\end{aligned}
$$

For $\|\psi\|^2_{S_h\times S_h} = \frac{1}{C^2}\|W^{j-1}\|^2_{S_h} + \frac{\alpha^2}{2C\beta}\|\nabla Z^{j-1}\|^2_{S_h} + \frac{\beta^2}{2C\tau\gamma}\|\nabla W^{j-1}\|^2_{S_h} + C_1$, with an appropriate C_1 satisfying the fixed point theorem's criteria, it follows that $(\mathcal{H}(\psi), \psi)_{S_h\times S_h} > 0$. Thus, Brouwer fixed point theorem [4, 5, 17] guarantees a $\tilde{\psi} \in S_h \times S_h$ such that $\mathcal{H}(\tilde{\psi}) = 0$ and

$$
\|\tilde{\psi}\|_{S_h\times S_h} \leq \frac{1}{C^2}\|W^{j-1}\|^2_{S_h} + \frac{\alpha^2}{2C\beta}\|\nabla Z^{j-1}\|^2_{S_h} + \frac{\beta^2}{2C\tau\gamma}\|\nabla W^{j-1}\|^2_{S_h} + C_1.
$$

Choosing $(W^j, Z^j) = \tilde{\psi}$ with $\mathcal{H}(\tilde{\psi}) = 0$ satisfies equation (5.2), confirming the existence of (W^j, Z^j).

To establish uniqueness, let (W_1^j, Z_1^j) and (W_2^j, Z_2^j) be the two distinct pairs of solutions of (5.2). Choosing $X_w^j := W_1^j - W_2^j$ and $X_z^j := Z_1^j - Z_2^j$, we get

$$
(\delta_t X_w^j, \zeta) + \alpha(\nabla\delta_t X_z^j, \nabla\zeta) + \beta(\delta_t X_z^j, \zeta) = -(\boldsymbol{g}(W_1^j) - \boldsymbol{g}(W_2^j), \nabla\zeta) - \lambda(\nabla X_z^j, \nabla\zeta) - \gamma(X_z^j, \zeta), \tag{5.10a}
$$

$$
(\nabla X_w^j, \nabla\zeta') = (X_z^j, \zeta'). \tag{5.10b}
$$

We utilize the induction method again. Assume $X_w^{j-1} = X_z^{j-1} = 0$ aiming at proving that $X_w^j = X_z^j = 0$. Setting $\zeta = X_w^j$ in (5.10a) and $\zeta' = \delta_t X_z^j$, X_w^j, X_z^j in (5.10b), yields

$$
\frac{C_3}{2}\delta_t\Big(\|X_w^j\|_1^2 + \|X_z^j\|^2\Big) + \gamma\|\nabla X_w^j\|^2 + \lambda\|X_z^j\|^2 \leq C_4\Big(\|X_w^j\|^2 + \|\nabla X_w^j\|^2\Big). \tag{5.11}
$$

Here, we have also taken into account the fact that $\|\boldsymbol{g}(W_1^j) - \boldsymbol{g}(W_2^j)\| \leq C_5\|X_w^j\|$. Testing with $\zeta' = X_w^j$ in (5.10b) and then applying the Young's and Cauchy-Schwarz inequalities gives

$$
\|\nabla X_w^j\|^2 \leq C_6\big(\|X_w^j\|^2 + \|X_z^j\|^2\big). \tag{5.12}
$$

From equations (5.11) and (5.12), we have

$$
\delta_t\Big(\|X_w^j\|_1^2 + \|X_z^j\|^2\Big) \leq C\Big(\|X_w^j\|_1^2 + \|X_z^j\|^2\Big). \tag{5.13}
$$

Additionally, by using the definitions of $\delta_t\|X_w^j\|^2$ and $\delta_t\|X_z^j\|^2$, it follows that

$$\|X_w^j\|_1^2 + \|X_z^j\|^2 \leq \frac{1}{1-C\tau}\big(\|X_w^{j-1}\|_1^2 + \|X_z^{j-1}\|^2\big).$$

By choosing τ small enough to satisfy $1 - C\tau > 0$ and applying $X_w^{j-1} = X_z^{j-1} = 0$ yields $\|X_w^j\| = \|X_z^j\| = 0$. Hence, $X_w^j = X_z^j = 0$, establishing the uniqueness of (W^j, Z^j). □

Theorem 5.5 *Let (w, z) be the solution of (2.2) and (W, Z) the solution of the fully discrete scheme (5.2). Assume that $w \in L^\infty(0,T;H_0^1(\Omega)) \cap L^\infty(0,T;H^r(\Omega))$ with $w_t \in L^2(0,T;H^r(\Omega))$ and $w_{tt} \in L^2(0,T;L^2(\Omega))$. Additionally, assume that $z \in L^\infty(0,T;H_0^1(\Omega)) \cap L^\infty(0,T;H^r(\Omega))$ with $z_t \in L^2(0,T;H^{r+1}(\Omega))$, $z_{tt} \in L^2(0,T;H^1(\Omega))$, and $z(0) \in H^r(\Omega)$. Then, the following estimate holds true*

$$h\|w(t^J) - W^J\|_1 + \|z(t^J) - Z^J\| \leq C(T,\Omega,w,w_t,w_{tt},z,z_t,z_{tt})\,(h^r+\tau),\quad J = 1,2\ldots M,$$

where C denotes a positive constant independent of h and τ.

Proof We establish the proof in the following parts:

1. Projection Error Bounds. Let $j \in \{1,\ldots,M\}$. The error can be expressed as

$$w(t^j) - W^j = (w(t^j) - \Pi_h w(t^j)) + (\Pi_h w(t^j) - W^j) = \varrho^j + \vartheta^j,$$
$$z(t^j) - Z^j = (z(t^j) - \Pi_h z(t^j)) + (\Pi_h z(t^j) - Z^j) = \mu^j + \varphi^j.$$

Bounds for ϱ^j and μ^j are already given by (4.3a) and (4.3b). It remains to estimate the discrete errors ϑ^j and φ^j.

2. Error Equations. To this end, we subtract equation (5.2) from (2.2) to get

$$\begin{aligned}\big(\delta_t\vartheta^j,\zeta\big) + \alpha\big(\nabla\delta_t\varphi^j,\nabla\zeta\big) + \beta\big(\delta_t\varphi^j,\zeta\big) + \lambda\big(\nabla\varphi^j,\nabla\zeta\big) + \gamma\big(\varphi^j,\zeta\big)\\ = -\big(w_t(t^j) - \delta_t(\Pi_h w(t^j)),\zeta\big) - \alpha\big(\nabla z_t(t^j) - \nabla\delta_t(\Pi_h z(t^j)),\nabla\zeta\big)\\ - \beta\big(z_t(t^j) - \delta_t(\Pi_h z(t^j)),\zeta\big) - \gamma\big(\mu^j,\zeta\big) + \big(\boldsymbol{g}(W^j) - \boldsymbol{g}(w(t^j)),\nabla\zeta\big),\end{aligned} \tag{5.14a}$$

$$\big(\nabla\vartheta^j,\nabla\zeta'\big) = \big(\mu^j,\zeta'\big) + \big(\varphi^j,\zeta'\big). \tag{5.14b}$$

One may see that

$$\big(\delta_t\varphi^j,\zeta'\big) = \big(\delta_t\nabla\vartheta^j,\nabla\zeta'\big) - \big(\delta_t\mu^j,\zeta'\big). \tag{5.15}$$

Also, equation (5.14b) with $\zeta' = \delta_t\varphi^j$ yields

$$\big(\nabla\vartheta^j,\nabla\delta_t\varphi^j\big) = \delta_t\big(\mu^j,\varphi^j\big) - \big(\delta_t\mu^j,\varphi^{j-1}\big) + \big(\varphi^j,\delta_t\varphi^j\big). \tag{5.16}$$

Using equations (5.14b), (5.15), and (5.16) in (5.14a) with $\zeta = \zeta' = \vartheta^j$, we get

$$\begin{aligned}\big(\delta_t\vartheta^j,\vartheta^j\big) + \alpha\big(\varphi^j,\delta_t\varphi^j\big) + \beta\big(\delta_t\nabla\vartheta^j,\nabla\vartheta^j\big) + \lambda\|\varphi^j\|^2 + \gamma\|\nabla\vartheta^j\|^2\\ = \alpha\big(\delta_t\mu^j,\varphi^{j-1}\big) - \alpha\delta_t\big(\mu^j,\varphi^j\big) + \beta\big(\delta_t\mu^j,\vartheta^j\big) - \lambda\big(\mu^j,\varphi^j\big)\\ - \big(w_t(t^j) - \delta_t(\Pi_h w(t^j)),\vartheta^j\big) - \alpha\big(\nabla z_t(t^j) - \nabla\delta_t(\Pi_h z(t^j)),\nabla\vartheta^j\big)\\ - \beta\big(z_t(t^j) - \delta_t(\Pi_h z(t^j)),\vartheta^j\big) + \big(\boldsymbol{g}(W^j) - \boldsymbol{g}(w(t^j)),\nabla\vartheta^j\big).\end{aligned} \tag{5.17}$$

Thus, the definitions of $\delta_t\vartheta^j$ and $\delta_t\varphi^j$ and the Cauchy-Schwarz and Young's inequalities, already give

$$(\delta_t\vartheta^j,\vartheta^j) + (\delta_t\varphi^j,\varphi^j) + \big(\delta_t\nabla\vartheta^j,\nabla\vartheta^j\big) \geq \frac{1}{2}\delta_t\big(\|\vartheta^j\|_1^2 + \|\varphi^j\|^2\big).$$

Applying the above, we can transform equation (5.17) into

$$\begin{aligned}\frac{C}{2}\delta_t\big(\|\vartheta^j\|_1^2+\|\varphi^j\|^2\big) \le& \alpha\big(\delta_t\mu^j,\varphi^{j-1}\big)-\alpha\delta_t\big(\mu^j,\varphi^j\big)+\beta\big(\delta_t\mu^j,\vartheta^j\big)-\lambda(\mu^j,\varphi^j)\\ &-\big(w_t(t^j)-\delta_t(\Pi_h w(t^j)),\vartheta^j\big)-\beta\big(z_t(t^j)-\delta_t(\Pi_h z(t^j)),\vartheta^j\big)\\ &+\big(\boldsymbol{g}(W^j)-\boldsymbol{g}(w(t^j)),\nabla\vartheta^j\big)-\alpha\big(\nabla z_t(t^j)-\nabla\delta_t(\Pi_h z(t^j)),\nabla\vartheta^j\big).\end{aligned} \tag{5.18}$$

where $C=min\{1,\alpha,\beta\}$.

3. Term-by-Term Estimation: We now proceed by multiplying the above equation throughout by 2τ, taking the sum from $j=1$ to J (arbitrary but less or equal to N). Consider each term one at the time. First, note that

$$2\tau\sum_{j=1}^{J}\frac{C}{2}\delta_t\big(\|\vartheta^j\|_1^2+\|\varphi^j\|^2\big)\ge C(\|\vartheta^J\|_1^2+\|\varphi^J\|^2-\|\varphi^0\|^2),$$

given $\vartheta^0=0$. Then, we proceed to bound the first term in the right-hand side of (5.18):

$$2\tau\alpha\sum_{j=1}^{J}(\delta_t\mu^j,\varphi^{j-1})\le C\bigg(\tau\sum_{j=1}^{J}\|\delta_t\mu^j\|^2+\tau\sum_{j=1}^{J}\|\varphi^{j-1}\|^2\bigg).$$

Here,

$$\begin{aligned}\|\delta_t\mu^j\|^2=\|(\delta_t z(t^j)-\delta_t\Pi_h z(t^j))\|^2&=\left\|\frac{z(t^j)-\Pi_h z(t^j)}{\tau}-\frac{z(t^{j-1})-\Pi_h z(t^{j-1})}{\tau}\right\|^2\\ &=\tau^{-2}\left\|\int_{t^{j-1}}^{t^j}(I-\Pi_h)z_t(\cdot,s)ds\right\|^2\\ &\le\tau^{-1}\bigg(\int_{t^{j-1}}^{t^j}\|(I-\Pi_h)z_t(\cdot,s)\|^2ds\bigg)\\ &\le C\tau^{-1}h^{2r}\int_{t^{j-1}}^{t^j}\|z_t(\cdot,s)\|_r^2ds,\end{aligned} \tag{5.19}$$

having used (4.3b) to obtain the last inequality. For the second term, we have

$$2\tau\alpha\sum_{j=1}^{J}\delta_t(\mu^j,\varphi^j)=\alpha\big[(\mu^J,\varphi^J)-(\mu^0,\varphi^0)\big]\le C^*\|\varphi^J\|^2+C\big(\|\mu^J\|^2+\|\mu^0\|^2+\|\varphi^0\|^2\big),$$

for some constants C and C^* with $C^*<min\{1,\alpha,\beta\}$. The third term is bounded similarly to the first term, hence we omit the details. For the fourth term, we have

$$2\tau\lambda\sum_{j=1}^{J}(\mu^j,\varphi^j)\le\lambda\bigg(\tau\sum_{j=1}^{J}\|\mu^j\|^2+\tau\sum_{j=1}^{J}\|\varphi^j\|^2\bigg).$$

Similarly, the fifth term we have

$$2\tau\sum_{j=1}^{J}(w_t(t^j)-\delta_t(\Pi_h w(t^j)),\vartheta^j)\le\tau\sum_{j=1}^{J}\big(\|w_t(t^j)-\delta_t(\Pi_h w(t^j)\|^2+\|\vartheta^j\|^2\big).$$

Further,

$$\|w_t(t^j) - \delta_t(\Pi_h w(t^j))\|^2 \le 2\big(\|w_t(t^j) - \delta_t w(t^j)\|^2 + \|\delta_t w(t^j) - \delta_t(\Pi_h w(t^j))\|^2\big) =: 2(Q_1 + Q_2).$$

Using Taylor's theorem, we get

$$\begin{aligned} Q_1 &= \left\| w_t(t^j) - \frac{w(t^j) - w(t^{j-1})}{\tau} \right\|^2 = \tau^{-2} \left\| \int_{t^{j-1}}^{t^j} (s - t^{j-1}) w_{tt}(\cdot, s) ds \right\|^2 \\ &\le \left\| \int_{t^{j-1}}^{t^j} w_{tt}(\cdot, s) ds \right\|^2 \\ &\le \tau \int_{t^{j-1}}^{t^j} \|w_{tt}(\cdot, s)\|^2 ds. \end{aligned} \tag{5.20}$$

A computation analogous to that leading to (5.21) shows that

$$\|\delta_t w(t^j) - \delta_t(\Pi_h w(t^j))\|^2 \le C\tau^{-1} h^{2r} \int_{t^{j-1}}^{t^j} \|w_t(\cdot, s)\|_r^2 ds.$$

The sixth term can be bounded similarly. For the seventh term, we first fix $\zeta' = \vartheta^j$ in (5.14b) to get

$$\|\nabla \vartheta^j\|^2 \le (\|\vartheta^j\|^2 + 2\|\varphi^j\|^2 + \|\mu^j\|^2).$$

Now, using the Lipschitz continuity of g and the above equation provides

$$\begin{aligned} 2\tau \sum_{j=1}^{J} (\boldsymbol{g}(W^j) - \boldsymbol{g}(w(t^j)), \nabla \vartheta^j) &\le 2\tau \sum_{j=1}^{J} \|\boldsymbol{g}(W^j) - \boldsymbol{g}(w(t^j))\| \|\nabla \vartheta^j\| \\ &\le 2\tau \sum_{j=1}^{J} \big(\|\varrho^j\| + \|\vartheta^j\|\big) \|\nabla \vartheta^j\| \\ &\le 4\tau \sum_{j=1}^{J} (\|\vartheta^j\|^2 + \|\varphi^j\|^2 + \|\mu^j\|^2 + \|\varrho^j\|^2). \end{aligned}$$

Finally, the last term provides

$$\begin{aligned} 2\tau\alpha \sum_{j=1}^{J} (\nabla z_t(t^j) - \nabla \delta_t(\Pi_h z(t^j)), \nabla \vartheta^j) &\le \alpha\tau \sum_{j=1}^{J} \big(\|\nabla z_t(t^j) - \nabla \delta_t(\Pi_h z(t^j)\|^2 + \|\nabla \vartheta^j\|^2\big) \\ &\le \alpha\tau \sum_{j=1}^{J} \big(2\|\nabla z_t(t^j) - \nabla \delta_t z(t^j)\|^2 + 2\|\nabla \delta_t z(t^j) - \nabla \delta_t(\Pi_h z(t^j))\|^2 + \|\nabla \vartheta^j\|^2\big) \end{aligned}$$

With a similar analysis to that conducted to obtain (5.19) and (5.20) we establish that

$$\|\nabla z_t(t^j) - \nabla \delta_t z(t^j)\|^2 \le \tau \int_{t^{j-1}}^{t^j} \|z_{tt}(\cdot, s)\|_1^2 ds,$$

$$\|\nabla \delta_t z(t^j) - \nabla \delta_t(\Pi_h z(t^j))\|^2 \le C\tau^{-1} h^{2r} \int_{t^{j-1}}^{t^j} \|z_t(\cdot, s)\|_{r+1}^2 ds.$$

Using all the above developments equations in (5.18), we conclude

$$\|\vartheta^J\|_1^2 + \|\varphi^J\|^2 \leq C(\|\varphi^0\|^2 + \|\mu^0\|^2) + C\tau \sum_{j=1}^{J}(\|\mu^j\|^2 + \|\varrho^j\|^2) + C\tau \sum_{j=0}^{J}(\|\vartheta^j\|^2 + \|\varphi^j\|^2)$$
$$+ Ch^{2r} \int_0^{t^J} \|z_t(\cdot, s)\|_{r+1}^2 ds + Ch^{2r} \int_0^{t^J} \|w_t(\cdot, s)\|_r^2 ds$$
$$+ C\tau^2 \int_0^{t^J} \|w_{tt}(\cdot, s)\|^2 ds + C\tau^2 \int_0^{t^J} \|z_{tt}(\cdot, s)\|_1^2 ds. \tag{5.21}$$

4. Application of Gronwall's Lemma. For estimating φ^0 above, fixing $\zeta' = \varphi^0$ in (5.14b) at initial level $j = 0$ gives

$$\left(\nabla\vartheta^0, \nabla\varphi^0\right) = \left(\mu^0, \varphi^0\right) + \left(\varphi^0, \varphi^0\right).$$

Thus, using once again Cauchy-Schwarz and Young's inequalities with $\vartheta^0 = 0$, we have

$$\|\varphi^0\|^2 \leq \|\mu^0\|^2 \leq Ch^{2r}\|z(0)\|_r^2. \tag{5.22}$$

Therefore, incorporating the given assumption with (5.21) yields

$$\|\vartheta^J\|_1^2 + \|\varphi^J\|^2 \leq C_1(h^{2r} + \tau^2) + C_2\tau \sum_{j=0}^{J}(\|\vartheta^j\|_1^2 + \|\varphi^j\|^2),$$

which we rewrite as

$$(1 - C_2\tau)\left[\|\vartheta^J\|_1^2 + \|\varphi^J\|^2\right] \leq C_1(h^{2r} + \tau^2) + C_2\tau \sum_{j=0}^{J-1}(\|\vartheta^j\|_1^2 + \|\varphi^j\|^2).$$

Choosing the time step τ such that $1 - C_2\tau > 0$, the discrete Gronwall's inequality provides

$$\|\vartheta^J\|_1^2 + \|\varphi^J\|^2 \leq C_1 \exp(C_2 T)(h^{2r} + \tau^2), \quad J = 1, 2, \ldots M. \tag{5.23}$$

The required a priori error bound now readily follows from (4.3a), (4.3b), and (5.23). □

6 Numerical Experiments

We report on a set of numerical tests assessing the convergence and conservation properties of the mixed finite element method.

The first two tests are designed to support the theoretical error bounds established in section 5. To assess convergence experimentally, we consider problems with known exact solution and compute the expected order of convergence (EOC) using the formula

$$\text{EOC} = \frac{\log\left(\frac{\|e_{j+1}\|}{\|e_j\|}\right)}{\log\left(\frac{h_{j+1}}{h_j}\right)},$$

where e_j denotes the error in a chosen norm at refinement level j and h_j is the corresponding mesh size.

All tests were performed with $\mathbb{P}_1 \times \mathbb{P}_1$ Lagrange finite elements on uniformly refined triangular meshes using the DUNE library [9, 21], except for the first test case, where $\mathbb{P}_2 \times \mathbb{P}_2$ Lagrange finite elements were used to assess higher-order accuracy.

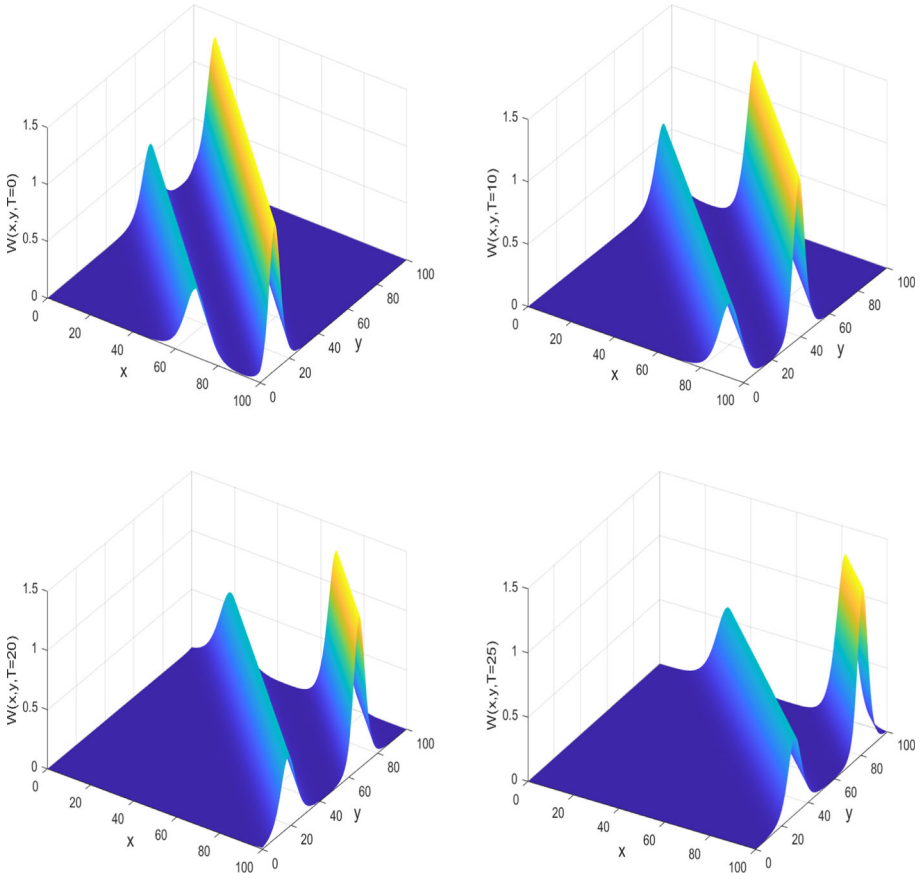

Fig. 1 Example 6.1. Evolution of two waves on a 200×200 grid with time step $\tau = 0.1$: computed solution at $T = 0, 10, 20, 25$

6.1 Interaction of Two Waves

Let $\Omega = [0, 100]^2$, $\alpha = \beta = \gamma = \lambda = s = 1$ and consider a non-homogeneous version of the KdV-RRLW model (1.1) obtained by adding a forcing term so that the exact solution is given by

$$w(x, y, t) = \sum_{i=1}^{2} \frac{q_i}{2} \operatorname{sech}^2\Big[k_i\big(x + y - (x_i + y_i) - v_i t\big)\Big], \tag{6.1}$$

where

$$q_i = 3(v_i - 2), \quad k_i = \frac{\sqrt{q_i}}{2p_i}, \quad p_i = \sqrt{6v_i}.$$

We further set $v_1 = 2.4$, $v_2 = 2.86$, $x_1 = y_1 = 35$, and $x_2 = y_2 = 55$. The initial and boundary conditions (1.2)–(1.3) are also defined to be compatible with the exact solution. Table 1 reports the convergence history of the variables w and z in the L^2 and H^1 norms for $\mathbb{P}_1 \times \mathbb{P}_1$ elements with various spatial and temporal step sizes, specifically $\tau = 1/10,\ 1/40,\ 1/160,\ 1/640,\ 1/2560$. Similarly, Table 2 shows the corresponding con-

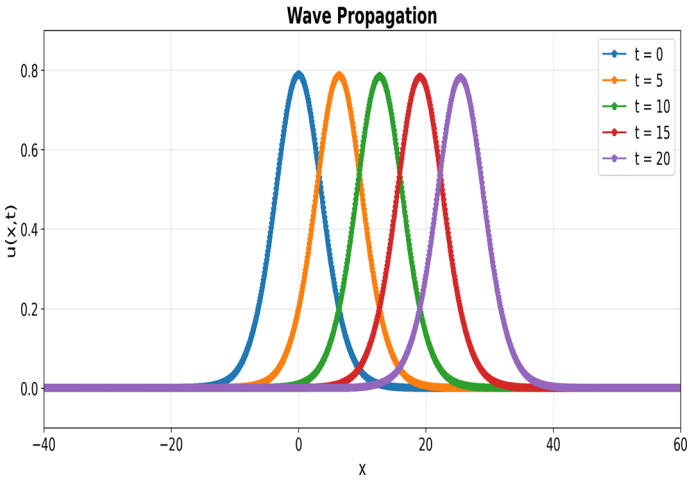

Fig. 2 Example 6.2. Evolution of a single wave traveling left-to-right. Initial profile and computed solution snapshots at $t = 5, 10, 15, 20$

vergence history for $\mathbb{P}_2 \times \mathbb{P}_2$ elements. Here, the time step τ is refined as $\tau \propto h^3$; each time h is halved, τ is reduced by a factor of 8. The values used are $\tau = 1/10, 1/80, 1/640, 1/5120$ corresponding to $h = 1/100, 1/200, 1/400, 1/800$, respectively. The observed rates are consistent with the theoretical results established in Theorem 5.5. Figure 1 illustrates the evolution of the two waves characterising the solution for $\tau = 0.1$ on a 200×200 grid at the final times $T = 0, 10, 20, 25$.

6.2 Propagation of 1D Solitary Wave

We consider the problem (1.1)–(1.3) in the one-dimensional setting on the domain $\Omega = [-40, 60]$ and with $T = 20$. The parameters are chosen as $\alpha = \beta = s = 1$ and $\gamma = \lambda = 0$. The initial condition is given by

$$w_0(x) = \frac{15}{19}\,\mathrm{sech}^4\left(\tfrac{\sqrt{13}}{26}x\right).$$

The corresponding exact solution takes the form [40]

$$w(x,t) = \frac{15}{19}\,\mathrm{sech}^4\left(\tfrac{\sqrt{13}}{26}\left(x - \tfrac{169}{133}t\right)\right).$$

Figure 2 illustrates the numerical solution computed with $h = 0.1$ and $\tau = 0.01$ using the proposed scheme, together with the exact solution at times $T = 0, 5, 10, 15, 20$.

To evaluate the performance of the present scheme, we benchmark it against the methods introduced in [40], which are based on a Crank–Nicolson type time-stepping. For fairness, we adapted our fully discrete formulation to also employ a Crank–Nicolson scheme, thereby allowing a direct comparison. In Table 3, we report L^2 errors and corresponding convergence rates for the step sizes $\tau = h$. In all cases, the present method yields marginally smaller and larger errors than Scheme I and II from [40], respectively.

Table 1 Example 6.1. Convergence history of both variables at $T = 1$ using $\mathbb{P}_1 \times \mathbb{P}_1$ elements

h, τ	$\|w(T) - W^M\|_{L^2}$	EOC	$\|w(T) - W^M\|_{H^1}$	EOC	$\|z(T) - Z^M\|_{L^2}$	EOC	$\|z(T) - Z^M\|_{H^1}$	EOC
$h = \frac{1}{100}, \tau = \frac{1}{10}$	8.9811×10^{-1}	–	8.7573×10^{-1}	–	3.3685×10^{-1}	–	4.6066×10^{-1}	–
$h = \frac{1}{200}, \tau = \frac{1}{40}$	2.3359×10^{-1}	1.94	3.9688×10^{-1}	1.14	8.9368×10^{-2}	1.91	2.0844×10^{-1}	1.14
$h = \frac{1}{400}, \tau = \frac{1}{160}$	5.8983×10^{-2}	1.98	1.9210×10^{-1}	1.04	2.2698×10^{-2}	1.97	1.0064×10^{-1}	1.05
$h = \frac{1}{800}, \tau = \frac{1}{640}$	1.4856×10^{-2}	1.99	9.4684×10^{-2}	1.02	5.7265×10^{-3}	1.99	4.9213×10^{-2}	1.03
$h = \frac{1}{1600}, \tau = \frac{1}{2560}$	3.7210×10^{-3}	2.00	4.7015×10^{-2}	1.01	1.4361×10^{-3}	2.00	2.4431×10^{-2}	1.01

Table 2 Example 6.1. Convergence history of both variables at $T = 1$ using $\mathbb{P}_2 \times \mathbb{P}_2$ elements.

h, τ	$\|w(T) - W^M\|_{L^2}$	EOC	$\|w(T) - W^M\|_{H^1}$	EOC	$\|z(T) - Z^M\|_{L^2}$	EOC	$\|z(T) - Z^M\|_{H^1}$	EOC
$h = \frac{1}{100}, \tau = \frac{1}{10}$	6.0959×10^{-1}	–	3.6257×10^{-1}	–	2.7117×10^{-1}	–	2.5103×10^{-1}	–
$h = \frac{1}{200}, \tau = \frac{1}{80}$	7.8570×10^{-2}	2.96	4.8049×10^{-2}	2.92	3.5430×10^{-2}	2.94	3.3852×10^{-2}	2.89
$h = \frac{1}{400}, \tau = \frac{1}{640}$	9.8893×10^{-3}	2.99	8.9521×10^{-3}	2.42	4.5182×10^{-3}	2.97	6.6245×10^{-3}	2.35
$h = \frac{1}{800}, \tau = \frac{1}{5120}$	1.2298×10^{-3}	3.00	1.9625×10^{-3}	2.19	5.5659×10^{-4}	3.00	1.4928×10^{-3}	2.14

Table 3 Example 6.2 Comparison of the accuracy of the current method and the method of [40] with step sizes $\tau = h$ at final time $T = 20$.

Present method			Pan et al. [40]			
$h = \tau$	L^2 error	EOC	L^2 error (Scheme I)	EOC	L^2 error (Scheme II)	EOC
0.4	2.6713×10^{-2}	–	2.85546×10^{-2}	–	2.43622×10^{-2}	–
0.2	6.7582×10^{-3}	1.98	7.27247×10^{-3}	1.97	6.17910×10^{-3}	1.98
0.1	1.6946×10^{-3}	2.00	1.82699×10^{-3}	1.99	1.55040×10^{-3}	1.99
0.05	4.2397×10^{-4}	2.00	4.57348×10^{-4}	2.00	3.87952×10^{-4}	2.00

6.3 2D Undular Bore [39]

An undular bore is a nonlinear wave phenomenon that arises when a disturbance propagates into a medium, generating a train of oscillatory waves. It is commonly modeled by taking $\beta = s = 1$ and $\alpha = \gamma = \lambda = 0$ in equations (1.1)–(1.3), with the initial condition

$$w_0(x, y) = \frac{1}{20}\left[1 - \tanh\left((x-a)^2 + (y-b)^2 - \zeta^2\right)\right],$$

where $\zeta = 2, a = b = 0$. The computational domain is chosen as $\Omega = [-60, 300]^2$ and final time is $T = 240$. We report the results obtained with the proposed finite element method setting $\tau = 0.1$ on a 501×501 uniform triangular computational grid. Figure 3 illustrates the evolution of the undular bore, showing its formation and subsequent propagation in the northeastward direction, which is consistent with the behavior reported in [39].

6.4 Maxwellian Initial Condition

The Maxwellian initial condition is a standard benchmark for testing numerical schemes for wave-type equations (see, e.g., [33, 39]). It provides a smooth, physically relevant profile that is useful for assessing the accuracy and stability of a method. It is also employed to model particle distributions in kinetic theory, where the density function follows a Gaussian profile. In our setting we take $\alpha = \beta = \gamma = \lambda = 1, s = 2$ in equations (1.1)–(1.3), with the initial condition

$$w(x, y, 0) = \exp\left(-\left((x-40)^2 + (y-40)^2\right)\right).$$

The space domain $\Omega = [0, 100]^2$ is discretized using a uniform triangular grid of size 200×200, and the simulation is advanced with a time increment of $\tau = 0.1$ until the final time $T = 20$. The resulting solution profiles are displayed in Figure 4, revealing the development of a wave pattern that propagates mainly toward the northeast.

6.5 Conservation Properties

In this last example, we investigate the properties established in Lemma 5.2 for the settings considered in Examples 6.2, 6.3 and 6.4. In addition to the quantities defined in (5.8), we also define

$$\tilde{E}(W^j) = \|W^j\|^2, \qquad \tilde{E}(W^j, Z^j) = \tilde{E}(W^j) + E(Z^j), \quad j = 1, \ldots, M. \tag{6.2}$$

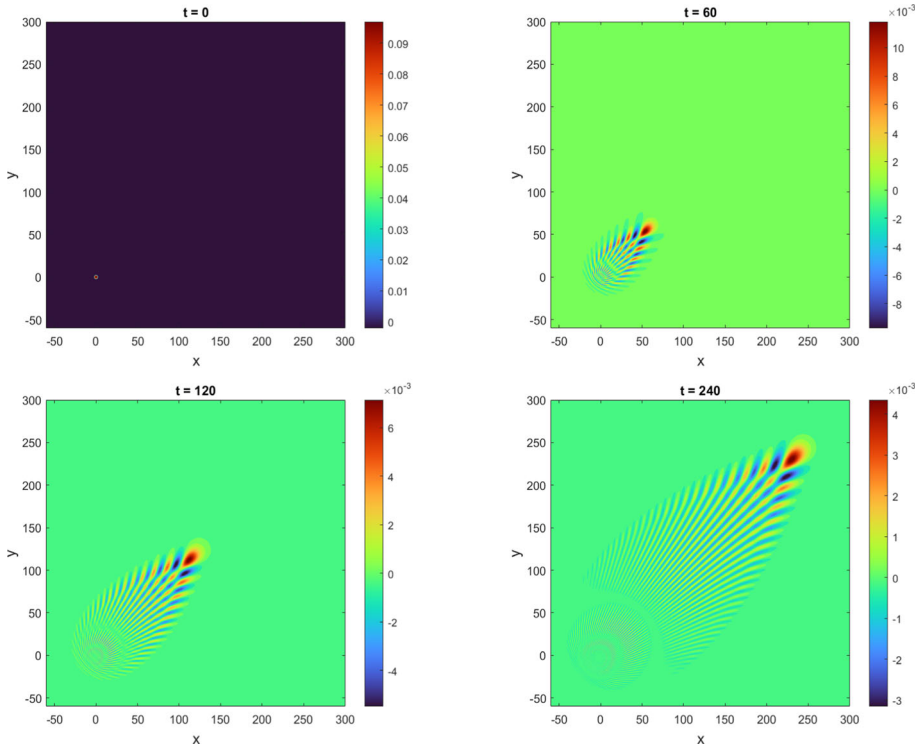

Fig. 3 Example 6.3. Evolution of the two-dimensional undular bore computed on a 501×501 grid with time step $\tau = 0.1$: initial and computed solution at $t = 60, 120, 240$

We track the temporal evolution of the discrete mass and energy quantities up to the final time T. and verify that the proposed numerical scheme preserves or dissipates these quantities in full agreement with the theoretical results.

Figure 5 illustrates the temporal evolution of the discrete mass and energy quantities for Example 6.2. In addition to tracking the structural properties, we now compare the discrete quantities with their exact counterparts and report the corresponding error profiles. As predicted by Lemma 5.2, the mass $M(W)$ remains constant throughout the simulation, while the energies evolve consistently with the discrete energy inequality (5.7). In particular, when $\gamma = \lambda = 0$ (Example 6.2), the dissipative terms vanish, and consequently the energy dissipation is negligible (see Figure 5). These observations confirm that the proposed numerical scheme accurately reproduces the conservation and dissipation mechanisms inherent to the continuous problem.

Figure 6 extends this analysis to the two-dimensional cases of Examples 6.3 and 6.4. Here, the time evolution of the mass and energy quantities demonstrates that the scheme continues to preserve or dissipate these structural properties as expected.

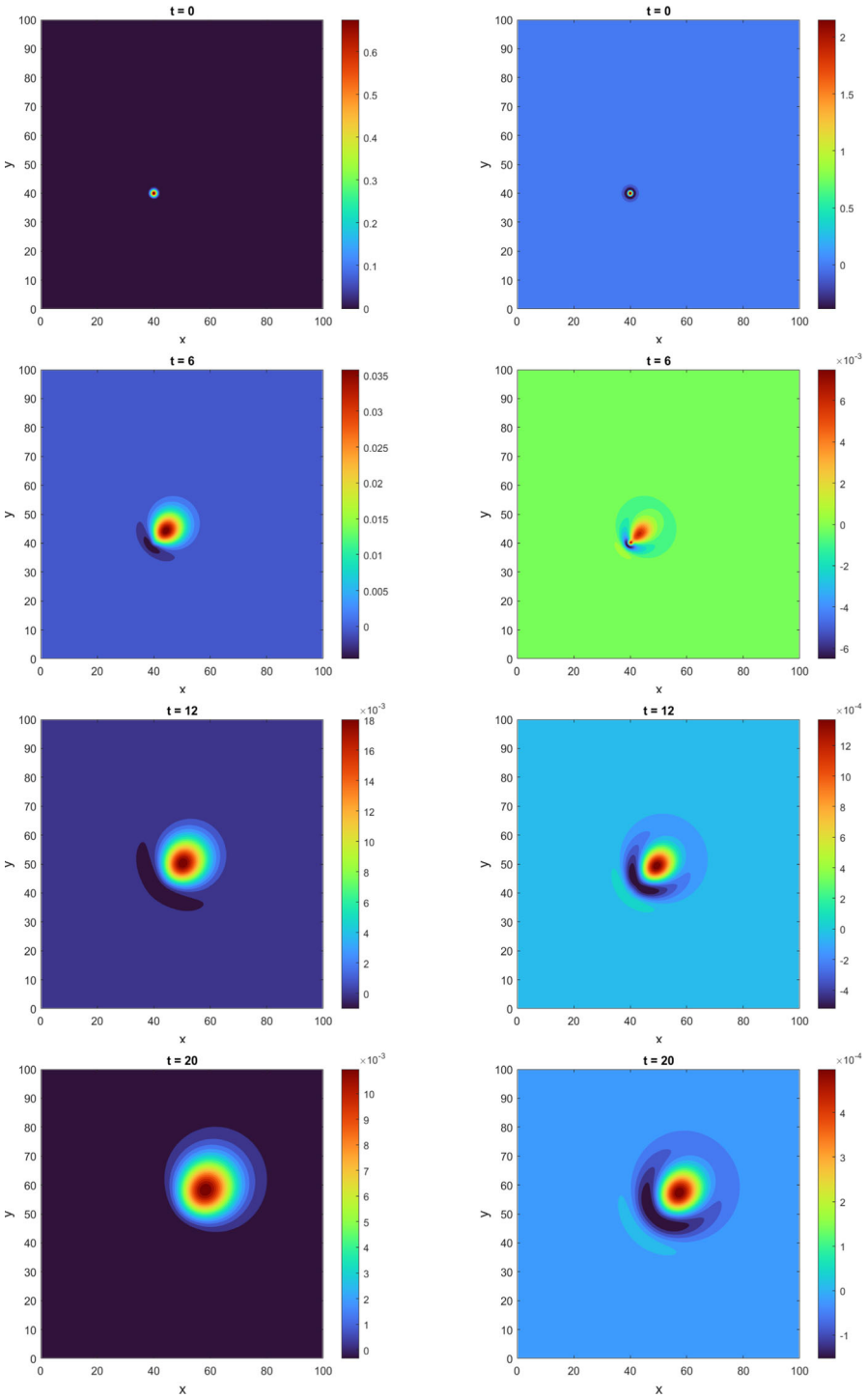

Fig. 4 Example 6.4. Numerical evolution of waves for w (left) and auxiliary variable z (right) for the Maxwellian initial condition on a 200×200 grid with time step $\tau = 0.1$: initial condition and computed solutions at $t = 6, 12, 20$

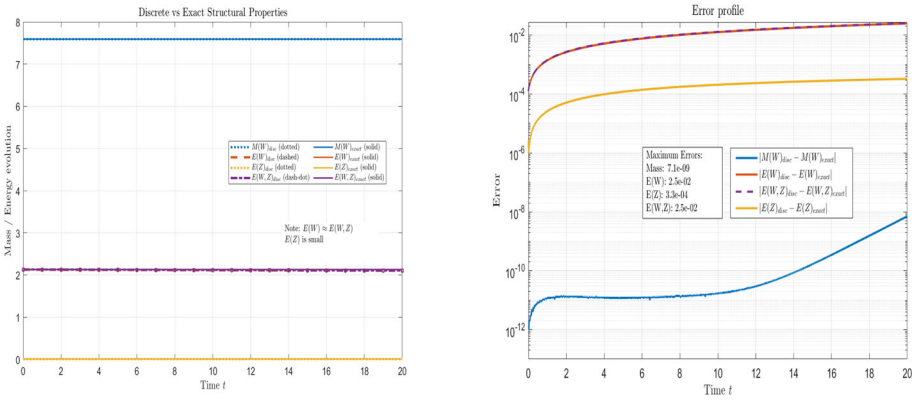

Fig. 5 Example 6.5. Verification of structural properties for Example 6.2. Left: comparison between exact and numerical values of the mass $M(W)$, the energies $E(W)$ and $E(Z)$, and the total energy $E(W, Z)$. Right: corresponding error profiles

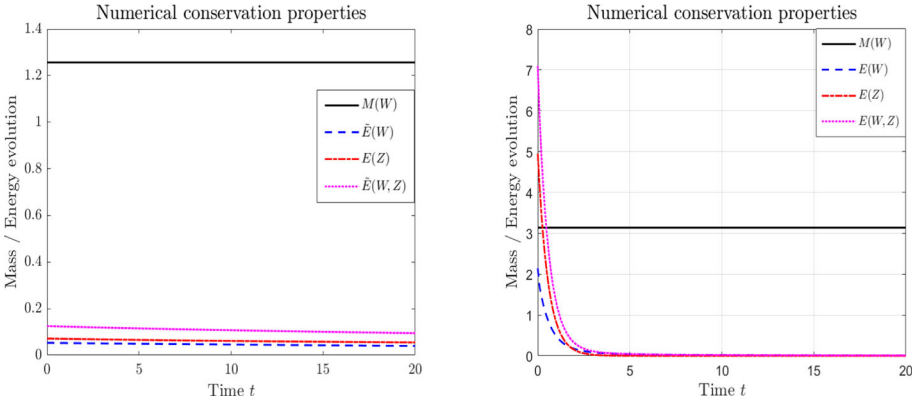

Fig. 6 Example 6.5. Time evolution of the mass and the energies for the setup in Example 6.3 (left) and Example 6.4 (right)

7 Conclusion

In this paper, we analyzed a conservative mixed finite element method for the nonlinear KdV–RRLW model containing a biharmonic term. We established the well-posedness of the decoupled system for the first time using Picard's existence and the Banach–Alaoglu theorems, supported by mass conservation and energy laws. Rigorous error estimates were derived: the semi-discrete scheme achieved optimal convergence in the H^1 and L^2 norms, while the fully discrete scheme was shown to be well-posed, mass-preserving, and energy-dissipative. Numerical experiments on benchmark problems confirmed these results, accurately capturing solitary waves, multi-wave interactions, undular bores, and Maxwellian-type solutions with optimal convergence rates. The future extension of our work involves deriving error estimates in H^1 Bôchner spaces and reducing the computational cost by using Polytopal methods.

Acknowledgements AC is member of INdAM Research group GNCS and acknowledges support by the European Union - NextGenerationEU, in the framework of the *iNEST - Interconnected Nord-Est Innovation Ecosystem* (iNEST ECS00000043 – CUP G93C22000610007) and European Union - Horizon Europe project *dealii-X: an Exascale Framework for Digital Twins of the Human Body* (Grant agreement ID: 101172493). RJ is thankful to ICTP and CIMPA for the CIMPA-ICTP Research in Pairs fellowships 2024 funding his research visit in Trieste. We also thank the anonymous referees for their valuable comments and suggestions.

Funding Open access funding provided by Scuola Internazionale Superiore di Studi Avanzati - SISSA within the CRUI-CARE Agreement.

Data Availability The authors will share the study data upon reasonable request.

Declarations

Competing interests The authors declare that they have no conflict of interest.

References

1. Abbaszadeh, M., Dehghan, M.: The interpolating element-free Galerkin method for solving Korteweg-de Vries-Rosenau-regularized long-wave equation with error analysis. Nonlinear Dyn. **96**, 1345–1365 (2019)
2. Ahlers, G., Cannell, D.S.: Vortex-front propagation in rotating Couette-Taylor flow. Phys. Rev. Lett. **50**, 1583 (1983)
3. Ainsworth, M., Andriamaro, G., Davydov, O.: Bernstein-Bézier finite elements of arbitrary order and optimal assembly procedures. SIAM J. Sci. Comput. **33**, 3087–3109 (2011)
4. Akrivis, G.D.: Finite difference discretization of the Kuramoto-Sivashinsky equation. Numer. Math. **63**, 1–11 (1992)
5. Jiwari, A.R., Kumar, N.: Analysis and simulation of Korteweg-de Vries-Rosenau-regularised long-wave model via Galerkin finite element method. Comput. Math. Appl. **135**, 134–148 (2023)
6. Aronson, D.G., Weinberger, H.F.: Multidimensional nonlinear diffusion arising in population genetics. Adv. Math. **30**, 33–76 (1978)
7. Babuška, I., Zlámal, M.: Nonconforming elements in the finite element method with penalty. SIAM J. Numer. Anal. **10**, 863–875 (1973)
8. Banz, L., Lamichhane, B.P., Stephan, E.P.: A new three-field formulation of the biharmonic problem and its finite element discretization, Numer Methods Partial. Differ. Equ. **33**, 199–217 (2017)
9. Bastian, P., Blatt, M., Dedner, A., Engwer, C., Klöfkorn, R., Kornhuber, R., Ohlberger, M., Sander, O.: A generic grid interface for parallel and adaptive scientific computing. Part II: implementation and tests in DUNE, Computing **82**, 121–138 (2008)
10. Behrens, E.M., Guzmán, J.: A mixed method for the biharmonic problem based on a system of first-order equations. SIAM J. Numer. Anal. **49**, 789–817 (2011)
11. Benjamin, T.B., Bona, J.L., Mahony, J.J.: Model equations for long waves in nonlinear dispersive systems. Philos. Trans. Roy. Soc. A **272**, 47–78 (1972)
12. Bialecki, B.: A fast solver for the orthogonal spline collocation solution of the biharmonic Dirichlet problem on rectangles. J. Comput. Phys. **191**, 601–621 (2003)
13. Bona, J.L., Smith, R.: The initial-value problem for the Korteweg-de Vries equation. Philos. Trans. Roy. Soc. A **278**, 555–601 (1975)
14. Brenner, S.C., Sung, L.Y.: C^0 interior penalty methods for fourth order elliptic boundary value problems on polygonal domains. J. Sci. Comput. **22**, 83–118 (2005)

15. Brenner, S.C., Sung, L.Y., Zhang, H., Zhang, Y.: A quadratic C^0 interior penalty method for the displacement obstacle problem of clamped Kirchhoff plates. SIAM J. Numer. Anal. **50**, 3329–3350 (2012)
16. Brezis, H., Brézis, H.: Functional analysis, Sobolev spaces and partial differential equations, vol. 2, Springer, (2011)
17. Browder, F.E.: Existence and uniqueness theorems for solutions of nonlinear boundary value problems, in Proceedings of symposia in applied mathematics, vol. 17, Providence: AMS, pp. 24–49 (1965)
18. Chung, S., Ha, S.: Finite element Galerkin solutions for the Rosenau equation. Appl. Anal. **54**, 39–56 (1994)
19. Ciarlet, P.G.: The finite element method for elliptic problems, SIAM, (2002)
20. Danumjaya, P., Pani, A.K.: Numerical methods for the extended Fisher-Kolmogorov (EFK) equation. J. Numer. Anal. Model. **3**, 186–210 (2006)
21. Dedner, A., Klöfkorn, R., Nolte, M., Ohlberger, M.: A generic interface for parallel and adaptive discretization schemes: abstraction principles and the DUNE-FEM module. Computing **90**, 165–196 (2010)
22. Dee, G., van Saarloos, W.: Bistable systems with propagating fronts leading to pattern formation. Phys. Rev. Lett. **60**, 2641 (1988)
23. Evans, L.C.: Partial differential equations, vol. 19, American Mathematical Society, (2022)
24. Falk, R.S.: Approximation of the biharmonic equation by a mixed finite element method. SIAM J. Numer. Anal. **15**, 556–567 (1978)
25. Girault, V., Raviart, P.-A.: Finite element methods for Navier-Stokes equations: theory and algorithms, vol. 5, Springer Science & Business Media, (2012)
26. Guo, H., Zhang, Z., Zou, Q.: A C^0 linear finite element method for biharmonic problems. J. Sci. Comput. **74**, 1397–1422 (2018)
27. Guozhen, Z.: Experiments on director waves in nematic liquid crystals. Phys. Rev. Lett. **49**, 1332 (1982)
28. Hornreich, R., Luban, M., Shtrikman, S.: Critical behavior at the onset of $\vec{k}$-space instability on the λ line. Phys. Rev. Lett. **35**, 1678 (1975)
29. Karageorghis, A., Fairweather, G.: The method of fundamental solutions for the numerical solution of the biharmonic equation. J. Comput. Phys. **69**, 434–459 (1987)
30. Kelmanson, M.: An integral equation method for the solution of singular slow flow problems. J. Comput. Phys. **51**, 139–158 (1983)
31. Kirby, R.C., Logg, A., Rognes, M. E., Terrel, A.R.: Common and unusual finite elements, in Automated Solution of Differential Equations by the Finite Element Method: The FEniCS Book, Springer, pp. 95–119 (2012)
32. Kirby, R.C., Mitchell, L.: Code generation for generally mapped finite elements. ACM Trans. Math. Softw. (TOMS) **45**, 1–23 (2019)
33. Lu, C., Huang, W., Qiu, J.: An adaptive moving mesh finite element solution of the regularized long wave equation. J. Sci. Comput. **74**, 122–144 (2018)
34. Ming, W., Xu, J.: The Morley element for fourth order elliptic equations in any dimensions. Numer. Math. **103**, 155–169 (2006)
35. Mohan, M.T., Khan, A.: On the generalized Burgers-Huxley equation: Existence, uniqueness, regularity, global attractors and numerical studies. Discrete Contin. Dyn. Syst. Ser. B **26**, 3943–3988 (2021)
36. Monk, P.: A mixed finite element method for the biharmonic equation. SIAM J. Numer. Anal. **24**, 737–749 (1987)
37. Nazarov, S., Sweers, G.: A boundary-value problem for the biharmonic equation and the iterated laplacian in a 3d-domain with an edge. J. Math. Sci. **143**, 2936–2960 (2007)
38. Omrani, K., Debebria, H., Bayarassou, K.: On the numerical solution of two-dimensional Rosenau–Burgers (RB) equation. Eng. With Comput **38**, 715–726 (2022)
39. Oruç, Ö.: An extrapolated second-order BDF combined with local Meshfree Radial Point Interpolation Method for numerical simulation of multi-dimensional Regularized Long Wave equation emerging in fluids: Ömer oruç. J. Sci. Comput. **104**, 44 (2025)
40. Pan, X., Zheng, K., Zhang, L.: Finite difference discretization of the Rosenau-RLW equation. Appl. Anal. **92**, 2578–2589 (2013)
41. Pandit, S.: A new algorithm for analysis and simulation of (2+1) Korteweg-de Vries-Rosenau-regularized long-wave model. Comput. Appl. Math. **43**, 35 (2024)
42. Quarteroni, A.: Numerical models for differential problems, vol. 2, Springer, 2009
43. Rosenau, P.: A quasi-continuous description of a nonlinear transmission line. Phys. Scr. **34**, 827 (1986)
44. Simon, J.: Compact sets in the space $L^p(0, T; B)$. Ann. Mat. Pura Appl. **146**, 65–96 (1986)
45. Stephenson, J.: Single cell discretizations of order two and four for biharmonic problems. J. Comput. Phys. **55**, 65–80 (1984)
46. Wang, M., Xu, J.: Minimal finite element spaces for $2m$-th-order partial differential equations in $\mathbb{R}^n$. Math. Comput. **82**, 25–43 (2013)

47. Zhang, S., Zhang, Z.: Invalidity of decoupling a biharmonic equation to two Poisson equations on non-convex polygons. Int. J. Numer. Anal. Model. **5**, 73–76 (2008)